Update on Dual Readout Calorimeter (DREAM) Project

Nural Akchurin (TTU)

Cagliari, Cosenza, ISU, Pavia, Pisa, Roma I, TTU

The Dual-Readout Calorimetry - I

- Combination of scintillation and Cherenkov radiators provides complimentary information about the composition of hadronic showers.

- The electromagnetic core of the hadronic showers is effectively sampled by clear (Cherenkov) fibers -- *e.g.* typically e/h~5 for quartz fiber calorimeters.

- The dual-readout technique is relatively simple if the two media (scintillator and clear radiators) are physically separated and read out by separate photosensors. The ratio of the two signals is a measure of the electromagnetic fraction, f_{em}, provided that the e/h ratios are known. This way, one of the dominating source of fluctuations can be measured event-by-event and thereby significantly improve the quality of energy measurement.

- The dual-readout technique is relatively difficult if the scintillation and Cherenkov light originate in the same medium.

The Dual-Readout Calorimetry - II

- We have carried out many tests using different types of crystals in the past few years to separate Cherenkov from scintillation light in order to apply the dual-readout idea to homogenous calorimeters.
- Fluctuations in the energy carried by neutrons, f_n, contribute to the energy resolution. It may be possible to better control these fluctuations and approach the ultimate limit in precision in hadron calorimetry.
- DREAM collaboration will continue to focus on generic calorimeter studies with an eye towards precision hadron calorimetry. Of course, we are interested in seeing that these development eventually finds meaningful applications in experiments.

DREAM Prototype

Basic structure:

$4x4\ mm^2$ Cu rods
2.5 mm radius hole
3 Sci. + 4 Clear fibers
Cu=69.3 : S=9.4 : C=12.6 :
Air=8.7
31.7% active/total filling fraction

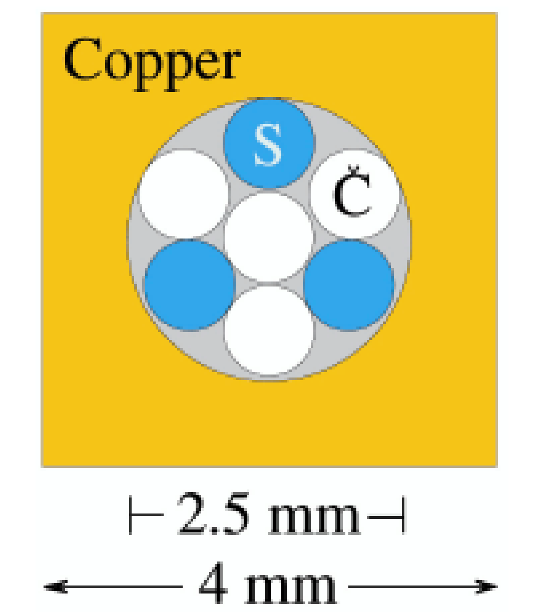

DREAM prototype:

5580 rods, 35910 fibers, 2 m long (10 λ_{int})
16.2 cm effective radius (0.81 λ_{int}, 8.0 ϱ_M)
1030 kg
X_0 = 20.10 mm, ϱ_M =20.35 mm
19 towers, 270 rods each
hexagonal shape, 80 mm apex to apex
Tower radius 37.10 mm (1.82 ϱ_M)
Each tower read-out by 2 PMs (1 for C and 1 for S fibers)
1 central tower + two rings

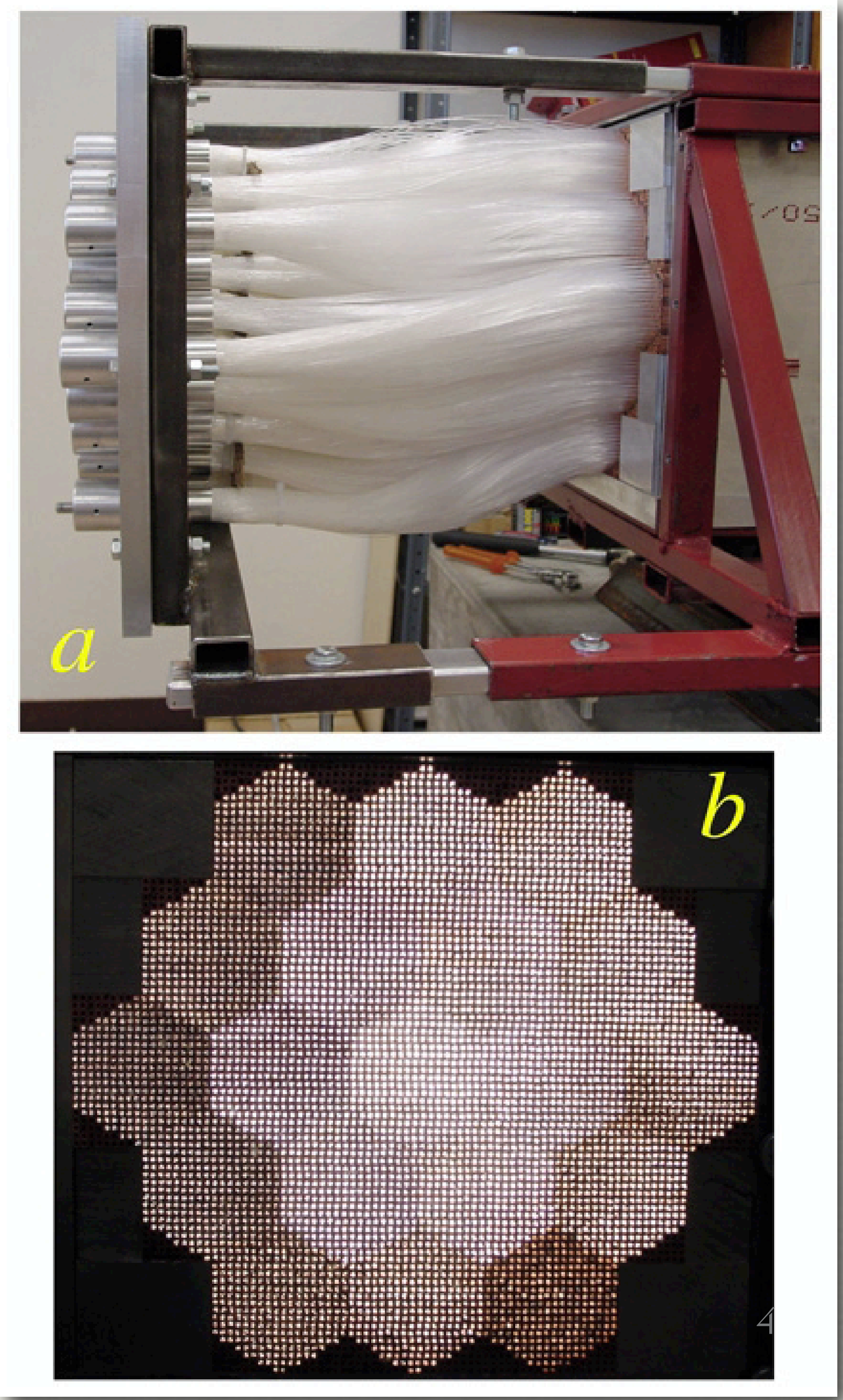

DREAM Prototype

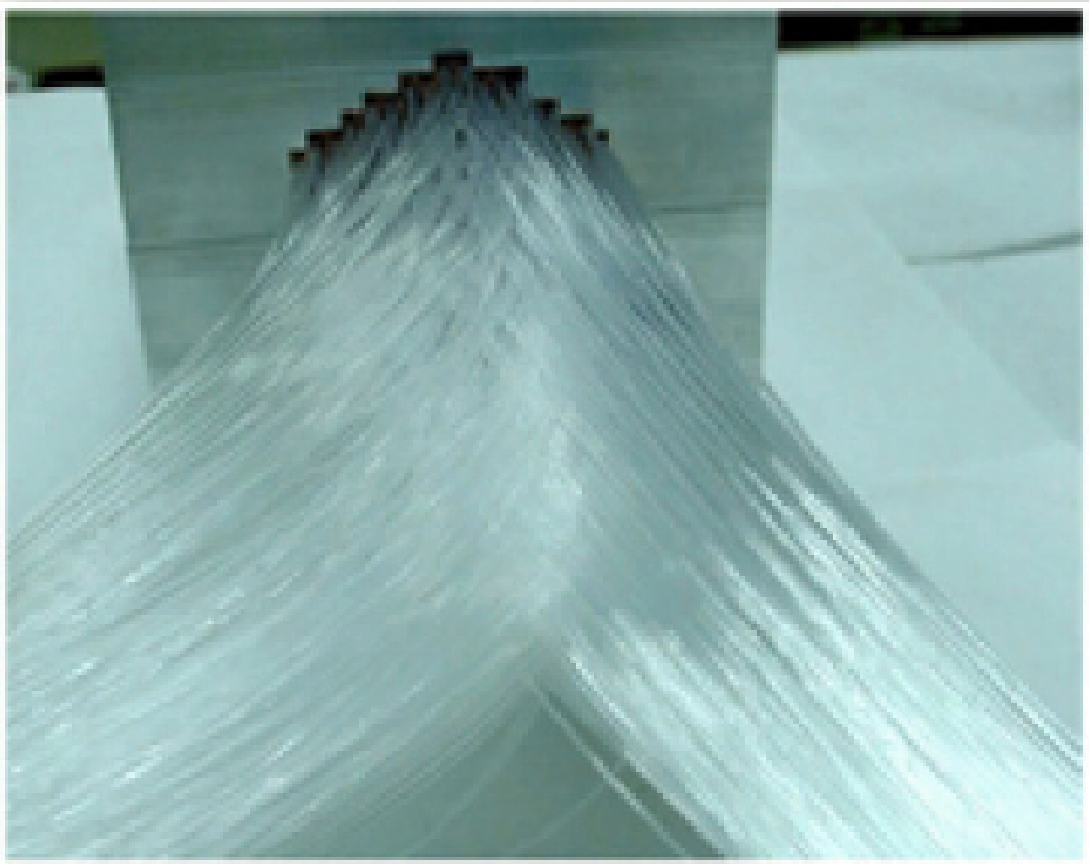

Beam tests:

CERN H4 beam line

Typical data samples:

pion/mu from 20 - 300 GeV

electrons 10 -150 GeV

“Jets” from 50 to 330 GeV

“Jets” mimicked by π interaction on 10 cm polyethylene target

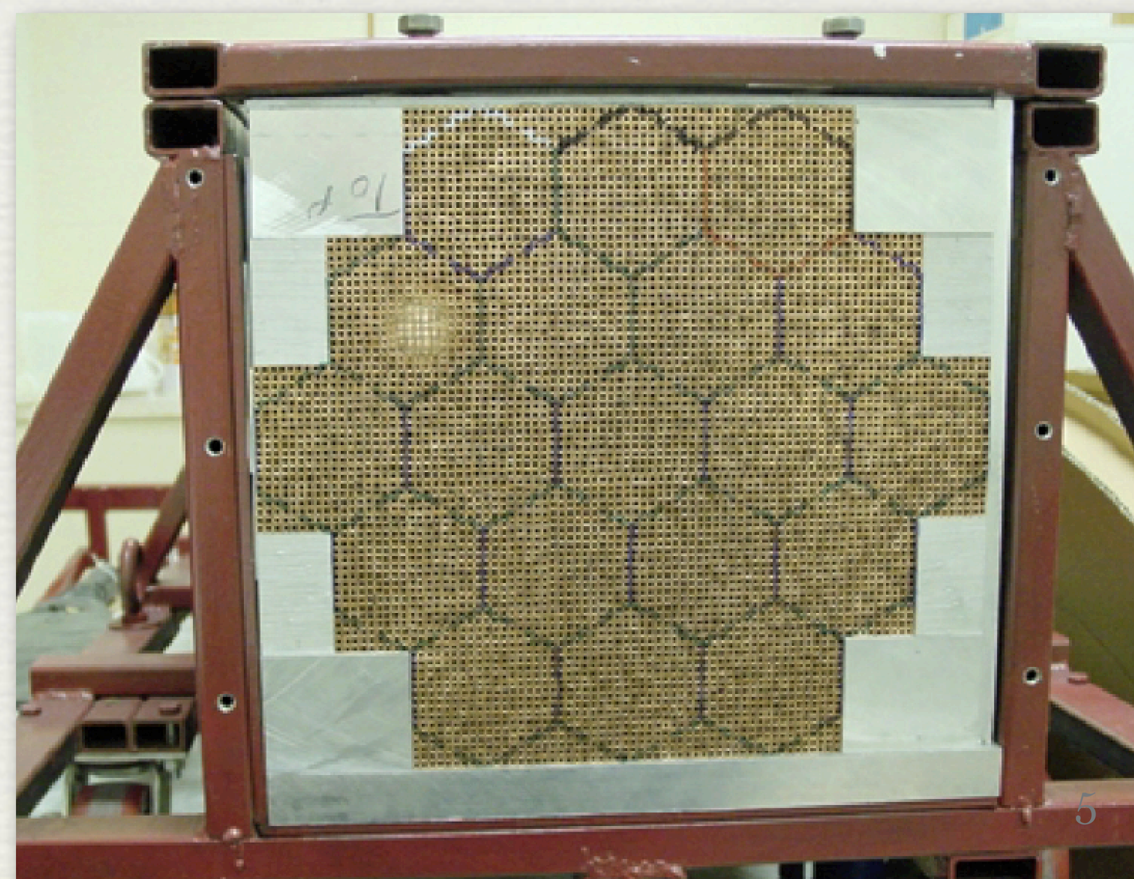

Radial Hadron Shower Profiles (DREAM)

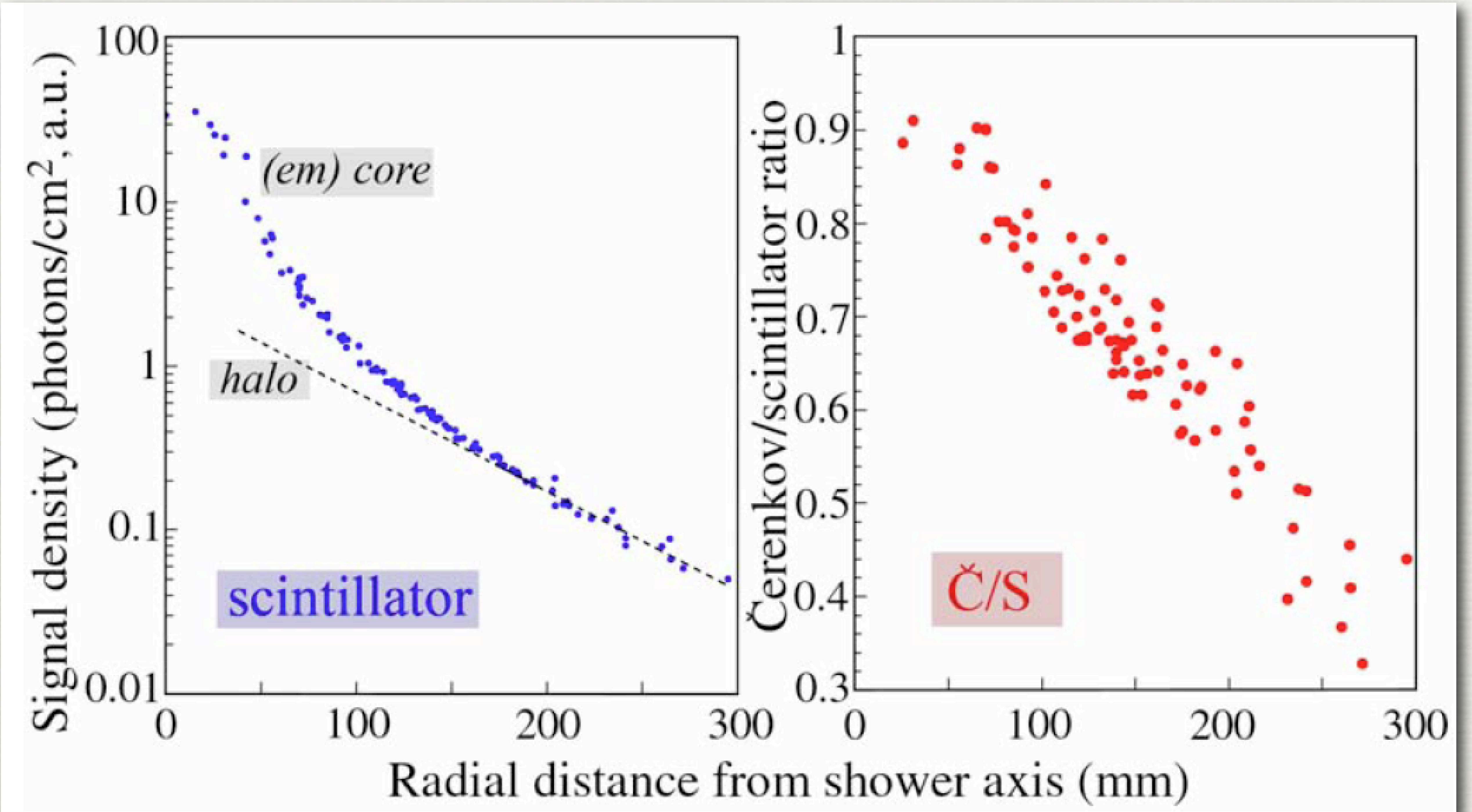

Calibration with 40 GeV Electrons

- Tilt 2° respect to the beam direction to avoid channelling effects
- Modest energy resolution for electrons (scintillator signal):

$$\frac{\sigma}{E} = \frac{20.5\%}{\sqrt{E}} + 1.5\%$$

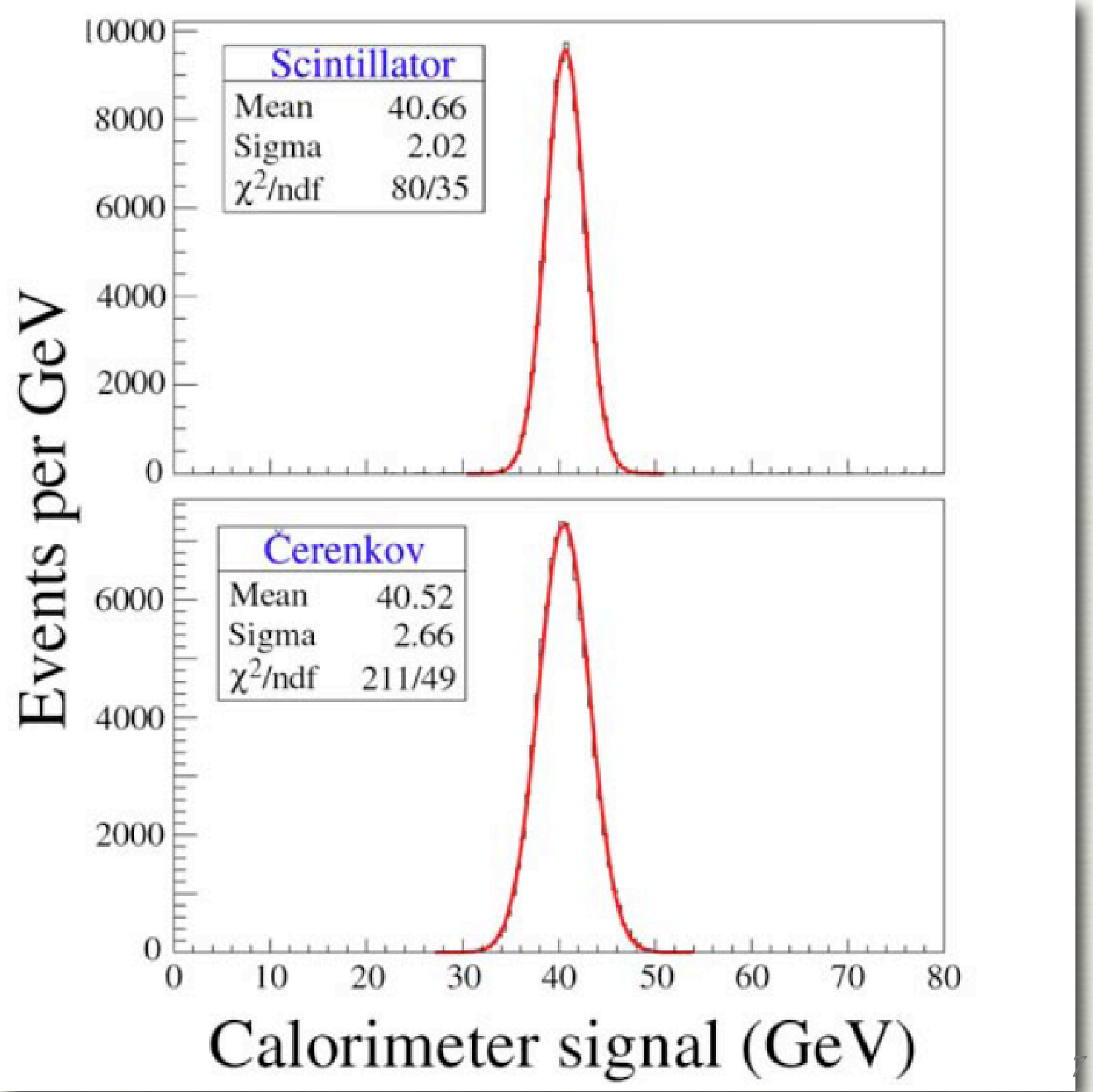

100 GeV Pions

- Signal distribution
  - Asymmetric, broad, smaller signal than for e⁻
  - Typical features of a non-compensating calorimeter

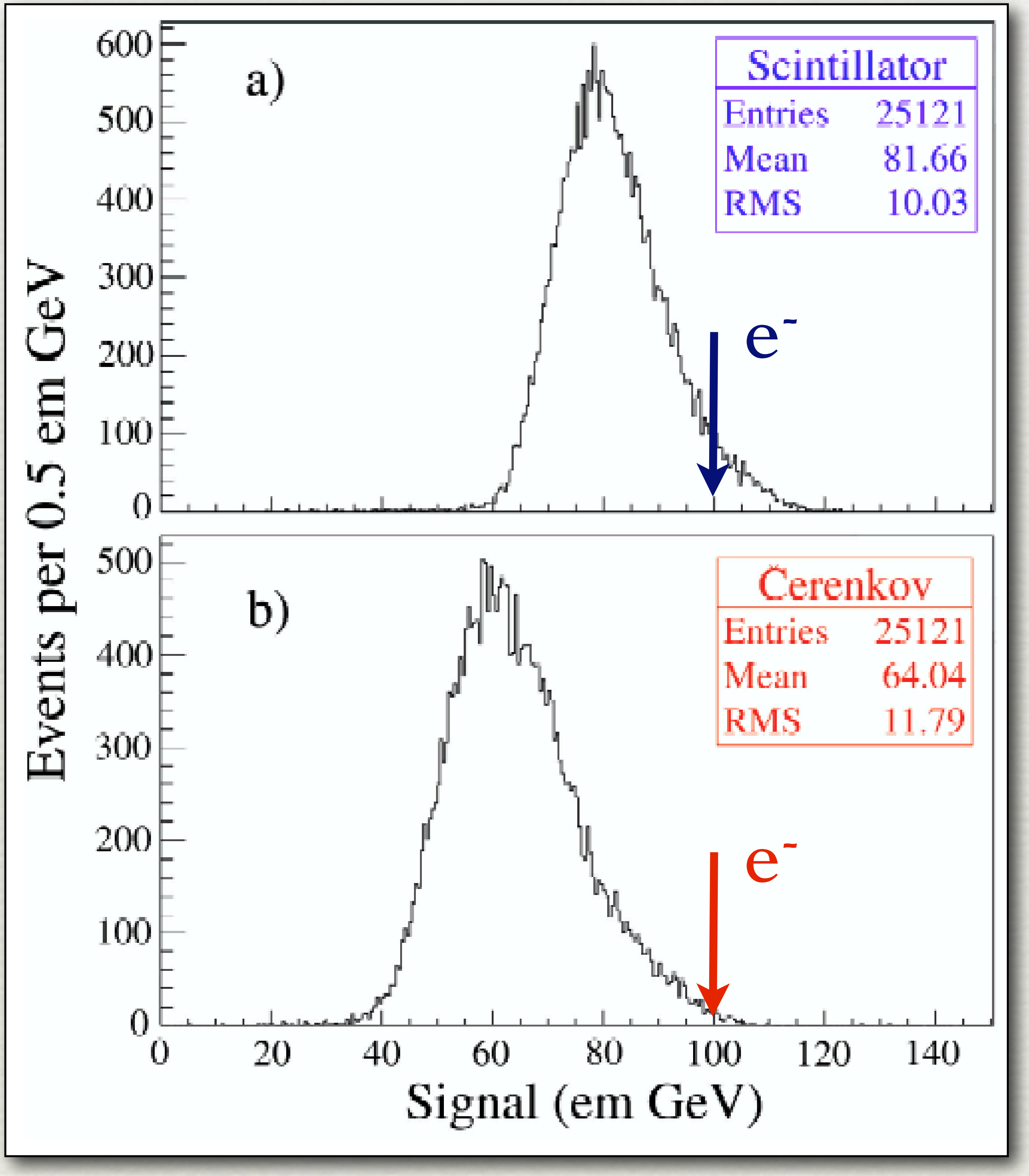

Hadronic Response (non-linearity)

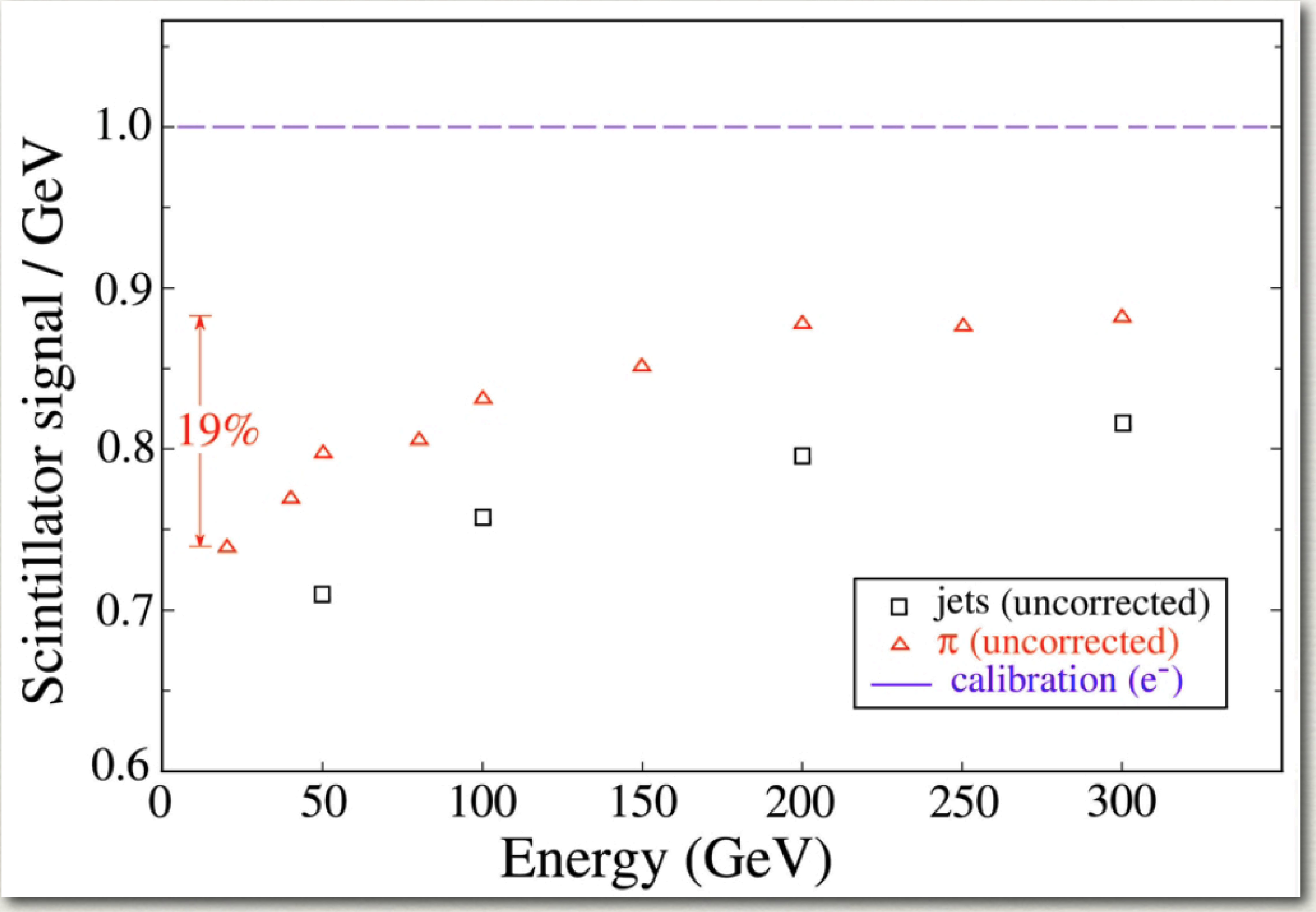

The (energy-independent) Q/S Method

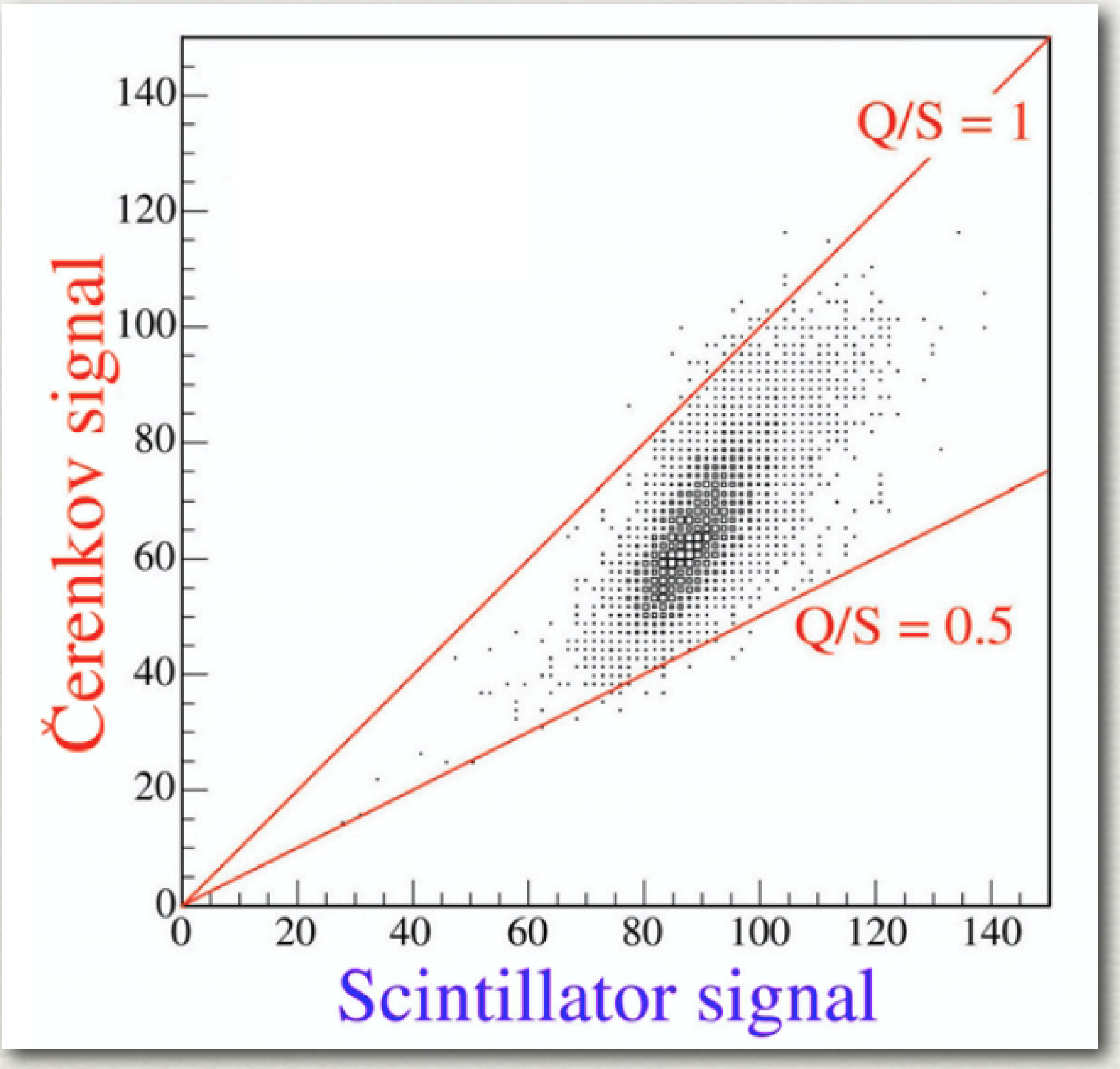

$$Q = E\left[f_{em} + \frac{1}{(e/h)_Q}(1 - f_{em}) \right]$$

$$S = E\left[f_{em} + \frac{1}{(e/h)_S}(1 - f_{em}) \right]$$

$$(e/h)_Q = 4.7$$

$$(e/h)_S = 1.3$$

$$\frac{Q}{S} = \frac{f_{em} + 0.21(1 - f_{em})}{f_{em} + 0.77(1 - f_{em})}$$

$$E = \frac{S - aQ}{1 - a}$$

$$a = \frac{1 - (h/e)_S}{1 - (h/e)_Q} \sim 0.3$$

Q/S ratio and f_{em}

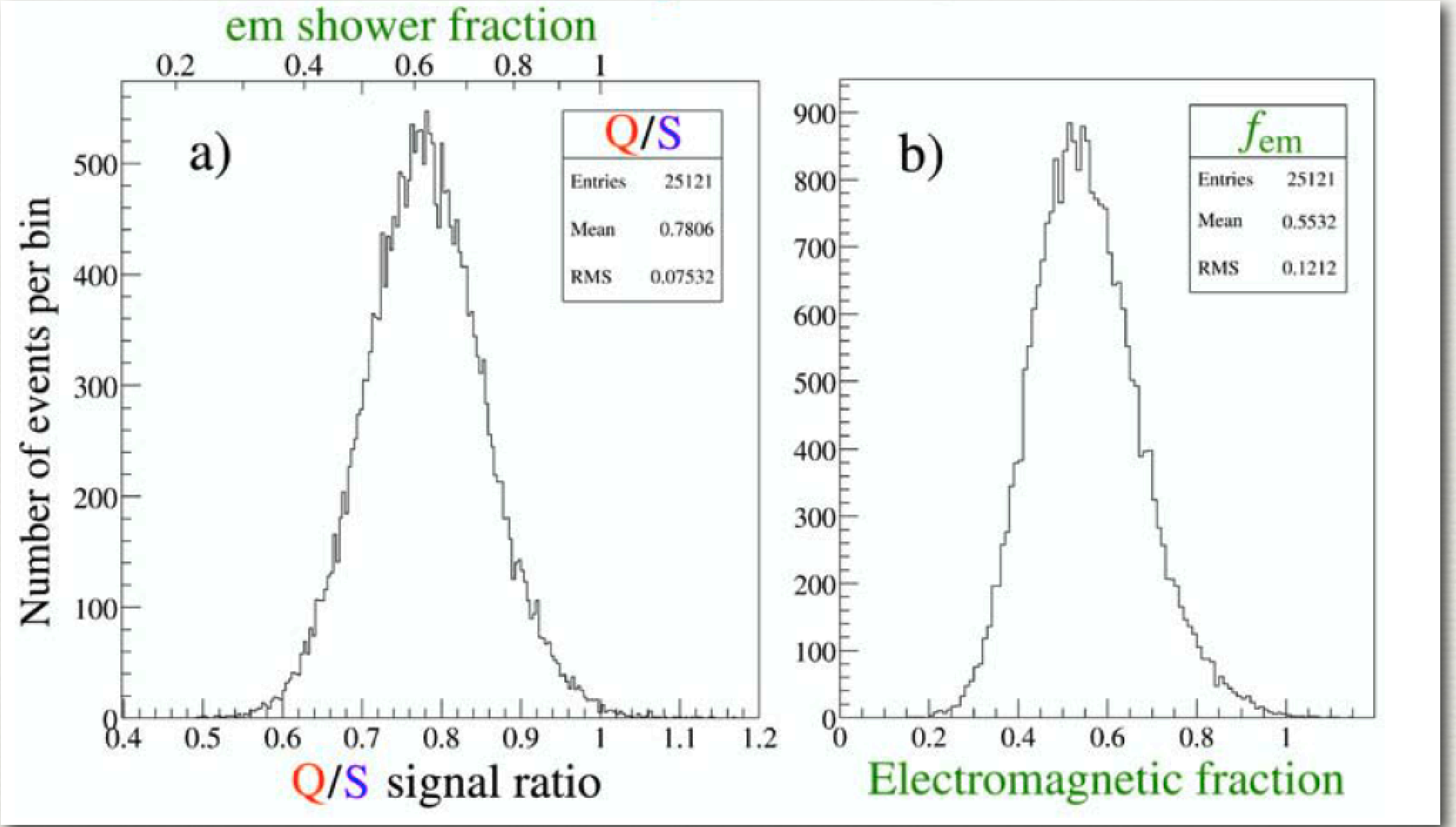

Total Signal and f_{em}

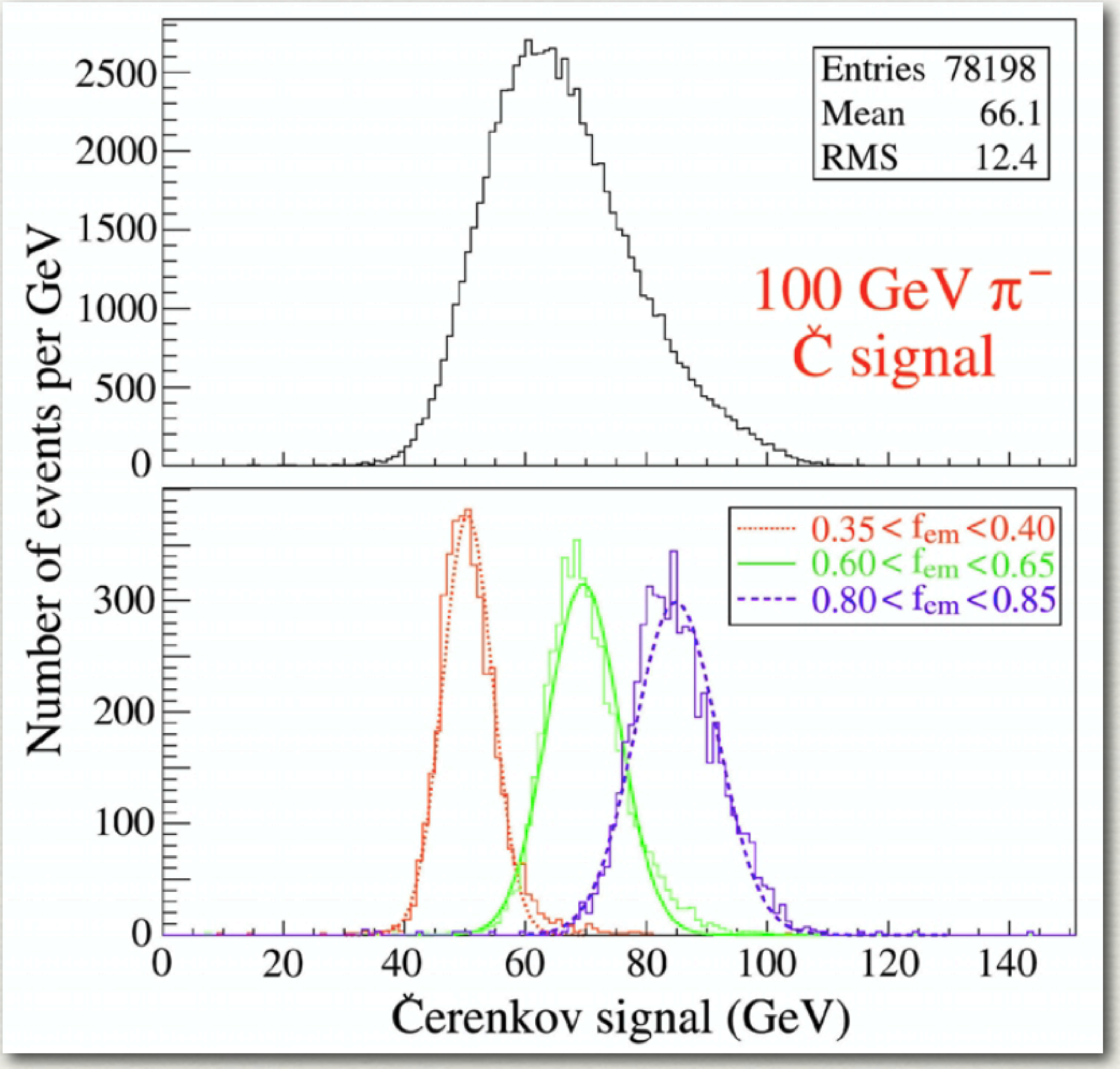

A Way to Measure e/h

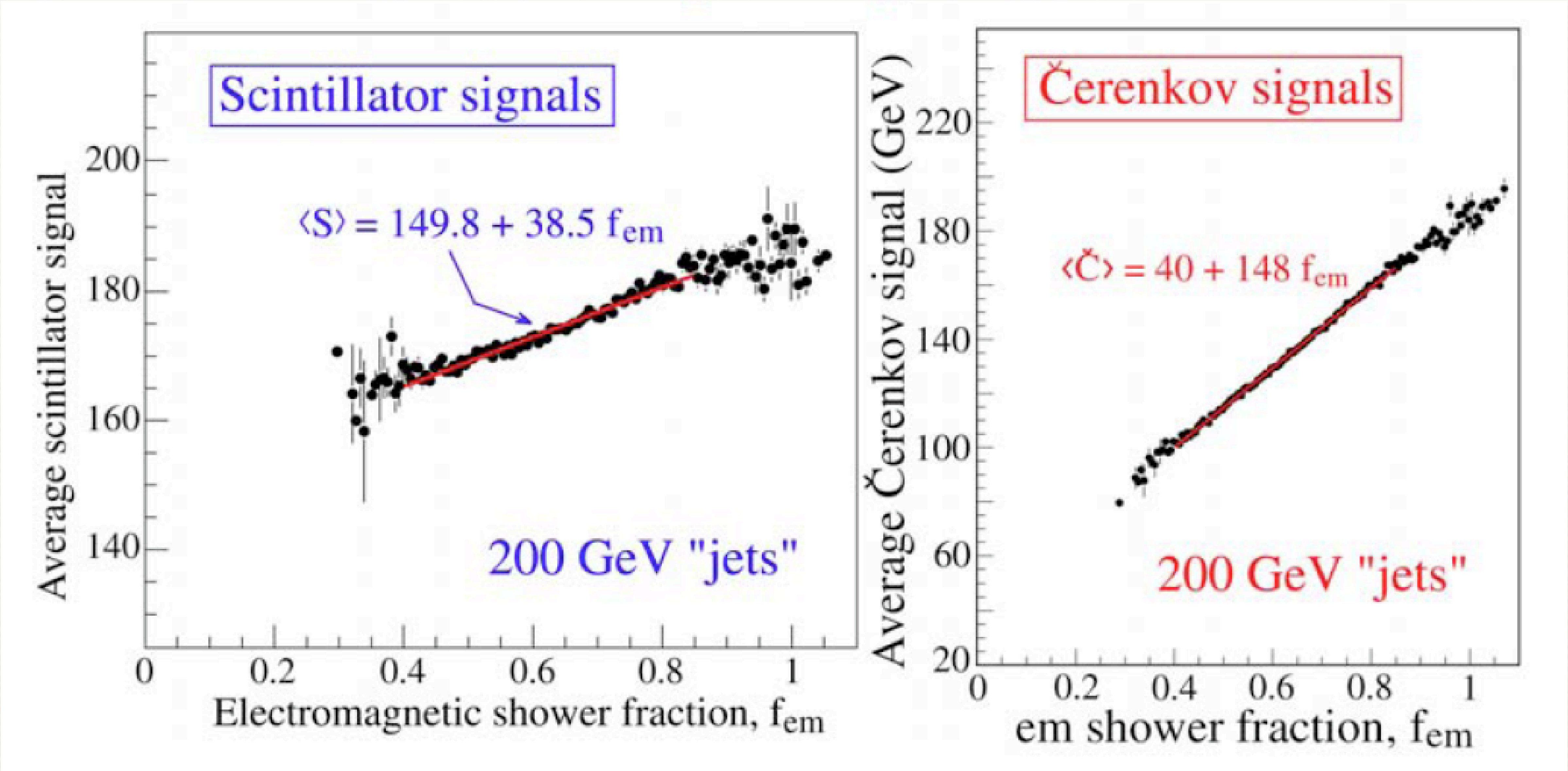

$$R(f_{em}) = p_0 + p_1 f_{em}$$

with

$$\frac{p_1}{p_0} = e/h - 1$$

Cu/scintillator e/h = 1.3

Cu/quartz e/h = 4.7

Dual-Readout Calorimetry in Practice

- The (energy-independent) Q/S method is followed with a signal correction method
- Each Cherenkov and scintillation signal in a given event is scaled by a factor that depends on the em fraction and the e/h ratio

$$\frac{Q}{S} = \frac{f_{\mathrm{em}} + 0.21(1 - f_{\mathrm{em}})}{f_{\mathrm{em}} + 0.77(1 - f_{\mathrm{em}})}$$

$$(e/h)_{\mathrm{Q}} = 4.7$$

$$(e/h)_{\mathrm{S}} = 1.3$$

$$S_{\mathrm{corr}} = S_{\mathrm{meas}} \left[\frac{1 + p_1/p_0}{1 + f_{\mathrm{em}} \cdot p_1/p_0} \right]$$

$$p_1/p_0 = (e/h)_{\mathrm{S}} - 1$$

$$Q_{\mathrm{corr}} = Q_{\mathrm{meas}} \left[\frac{1 + p_1/p_0}{1 + f_{\mathrm{em}} \cdot p_1/p_0} \right]$$

$$p_1/p_0 = (e/h)_{\mathrm{Q}} - 1$$

Hadronic Response: Effect Q/S Correction

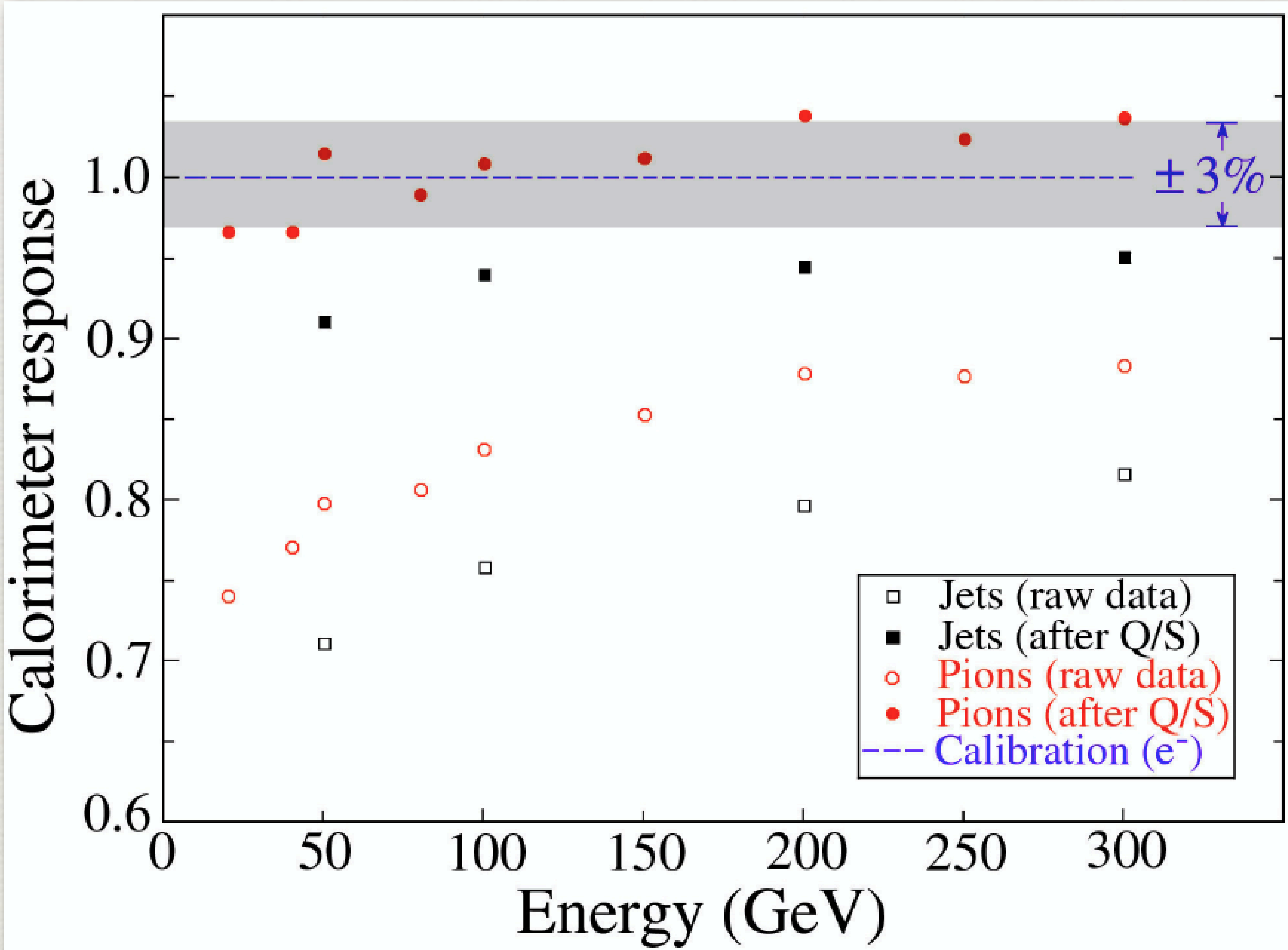

Effect of Corrections (200 GeV "jets")

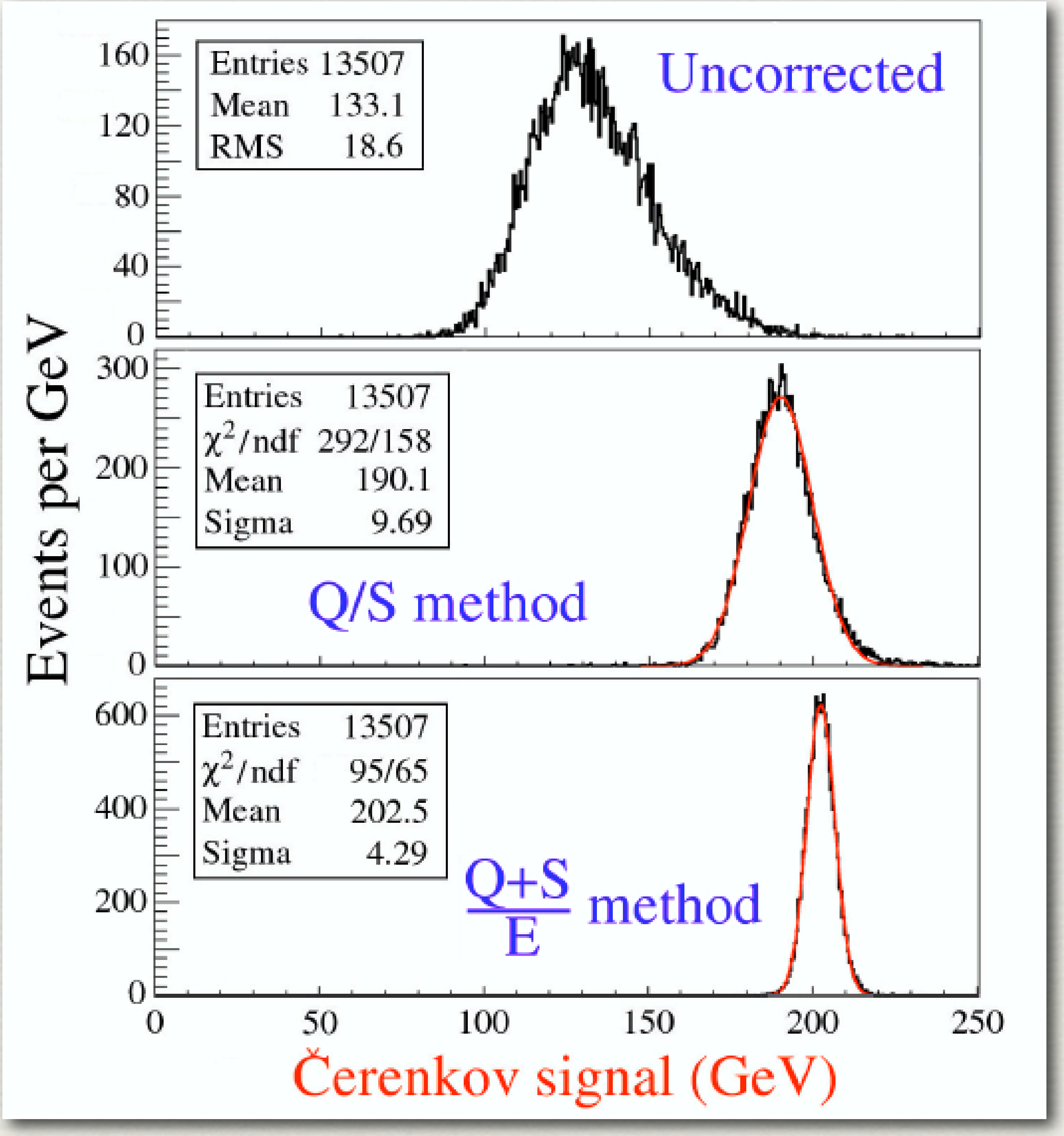

Energy Resolution for "jets"

- After corrections the energy resolution is dominated by leakage fluctuations

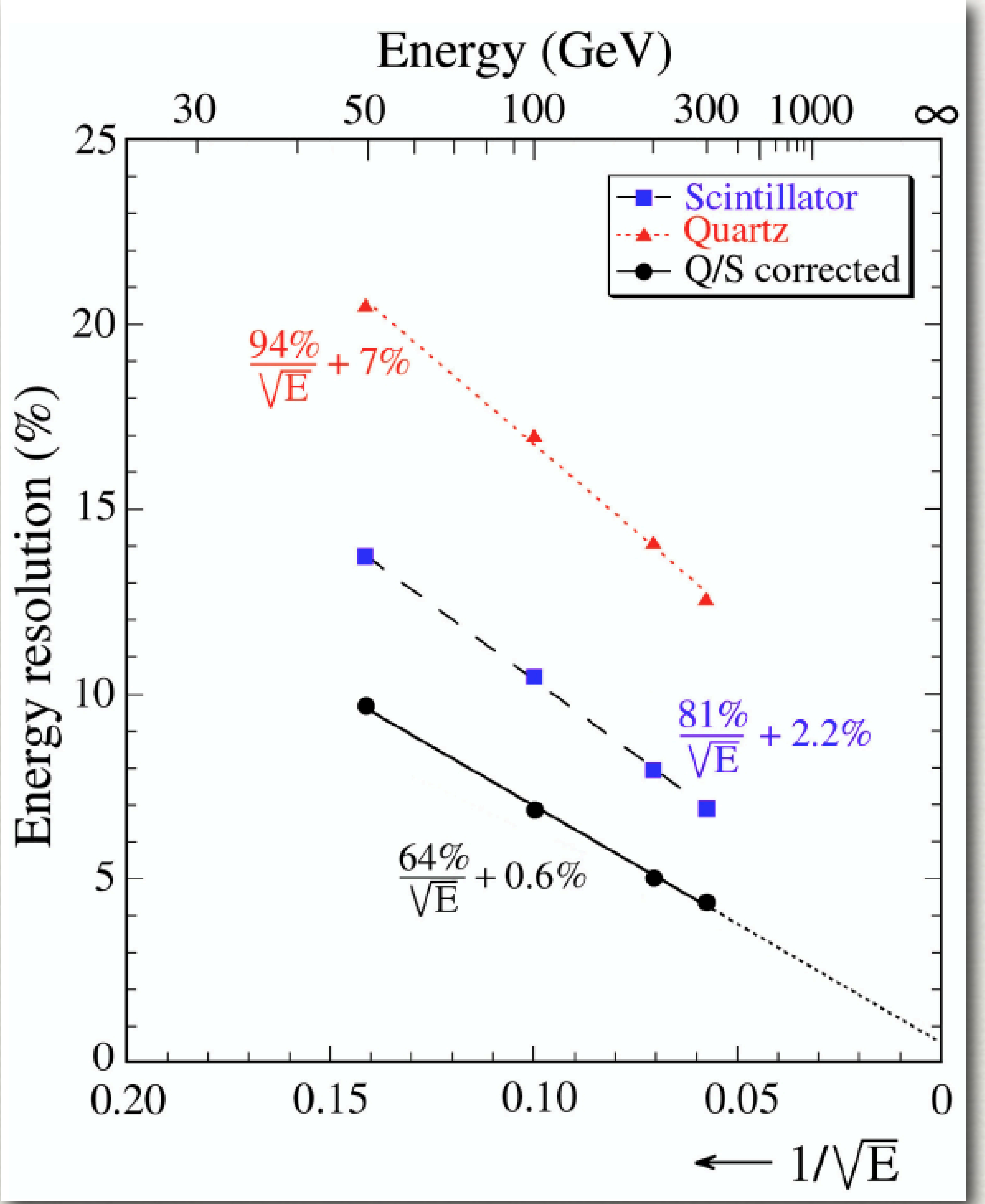

Lessons Learned with Fiber Dual Readout Calorimeter

- The dual-readout fiber calorimeter so far has taught us that it is possible to achieve compensation on an event-by-event basis.
- The hadronic signal distributions become symmetric.
- Correct energy scale can be obtained for hadrons and "jets" for a calorimeter calibrated with electrons.
- The hadronic energy resolution scales with $E^{-1/2}$.
- The DREAM prototype is only ~1 tonne and the leakage fluctuations are important.
- The Cherenkov light yield is a limiting factor at ~8 pe/GeV (~35%/$E^{1/2}$).
- Similar ideas may be applied to homogeneous calorimeters where S and C are separated by spectra, directionality, timing, polarization, *etc*...

Dual-readout with Crystals

- Lead Tungstate ($PbW0_4$): light yield ~10 pe/MeV and depends on temperature and readout. Expect sizable Cherenkov light.
- BGO ($Bi_4Ge_3O_{12}$)
    - Single crystal
    - Combined Calorimetry (Multicrystal BGO +DREAM)
- Doped $PbW0_4$
    - Molibdenum
    - Praesodymium

Lead Tungstate ($PbWO_4$) - I

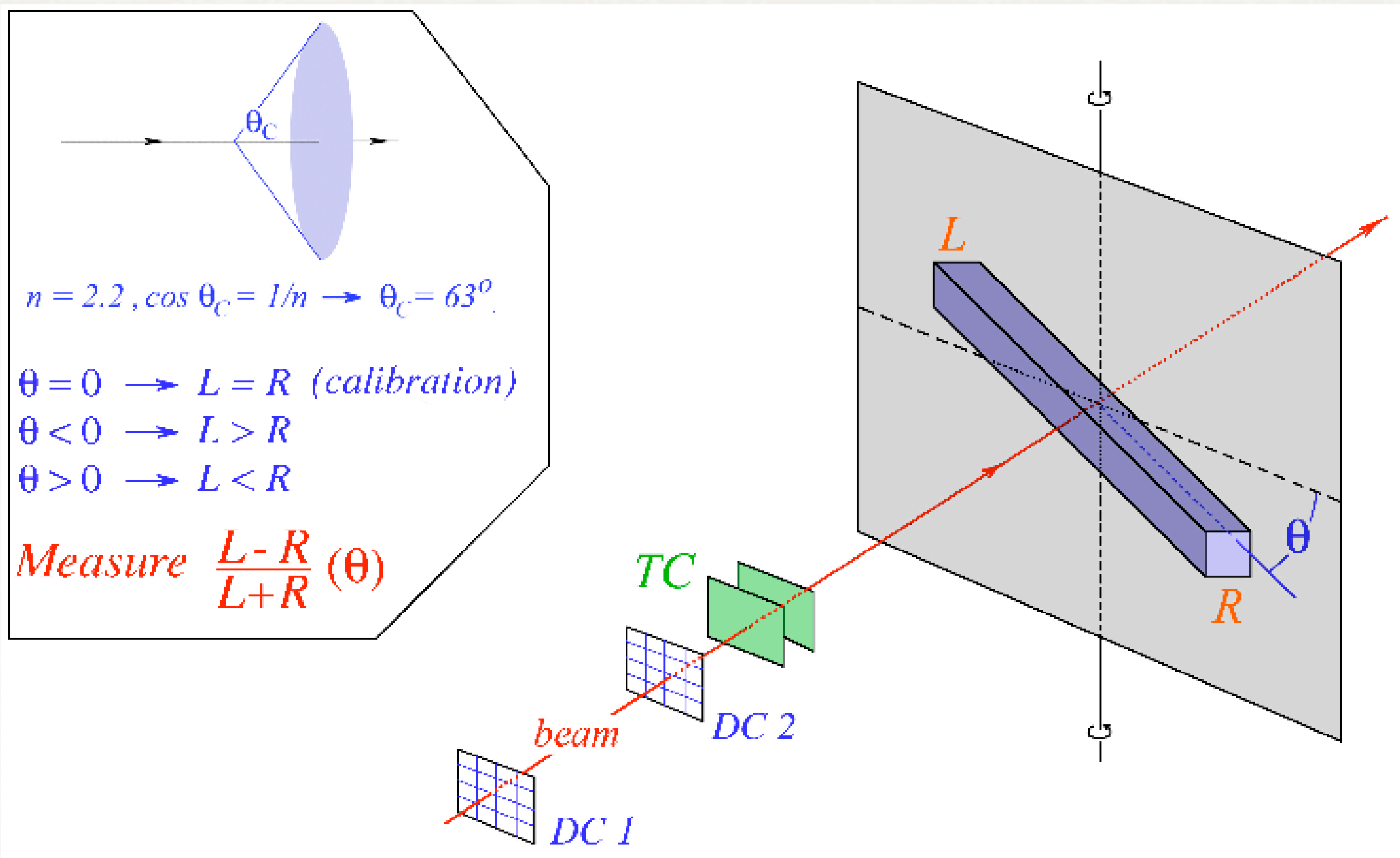

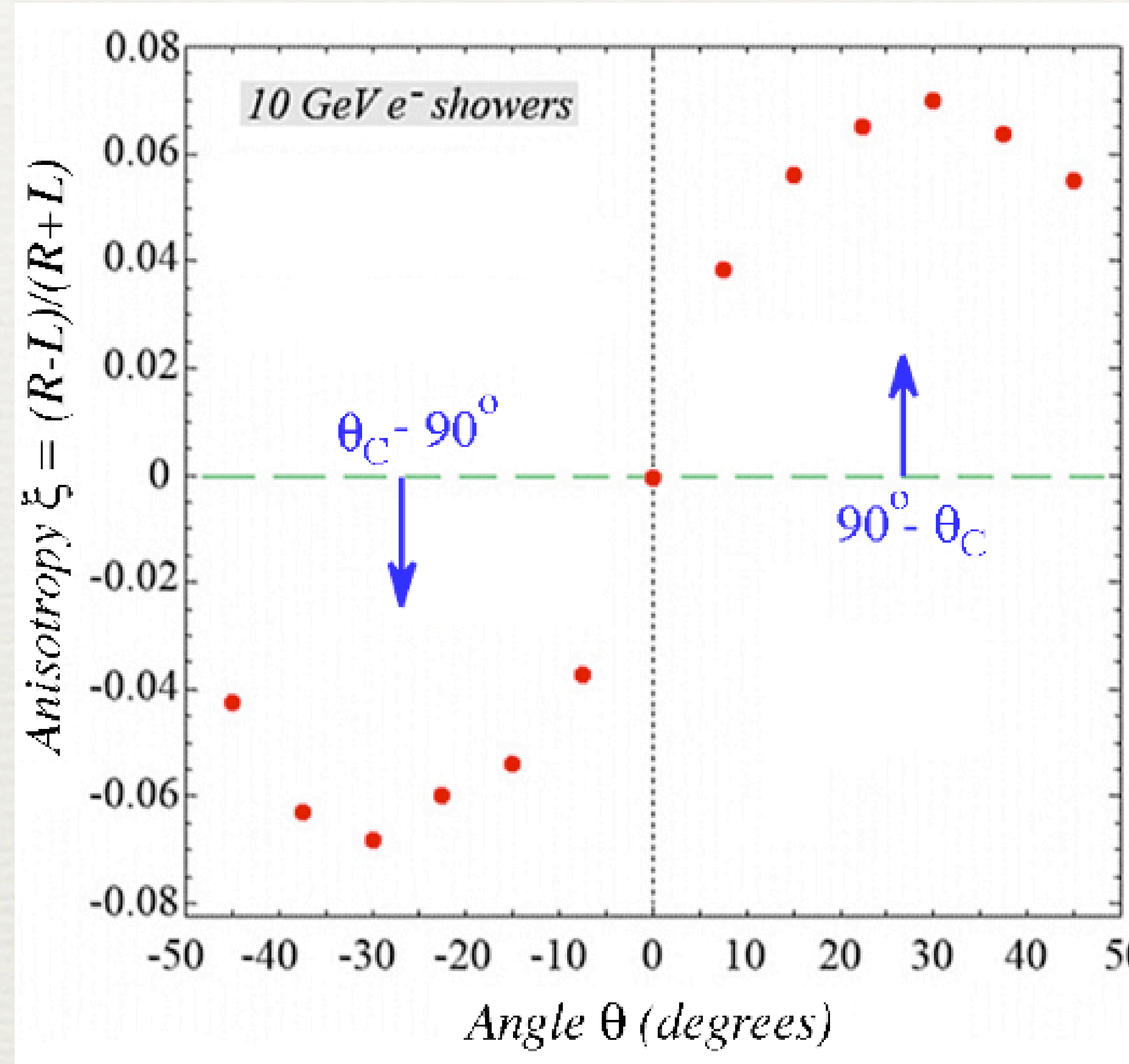

- Take advantage of directionality of Cherenkov light to observe asymmetry as a function of angle of incidence between Left and Right

Lead Tungstate ($PbWO_4$) - II

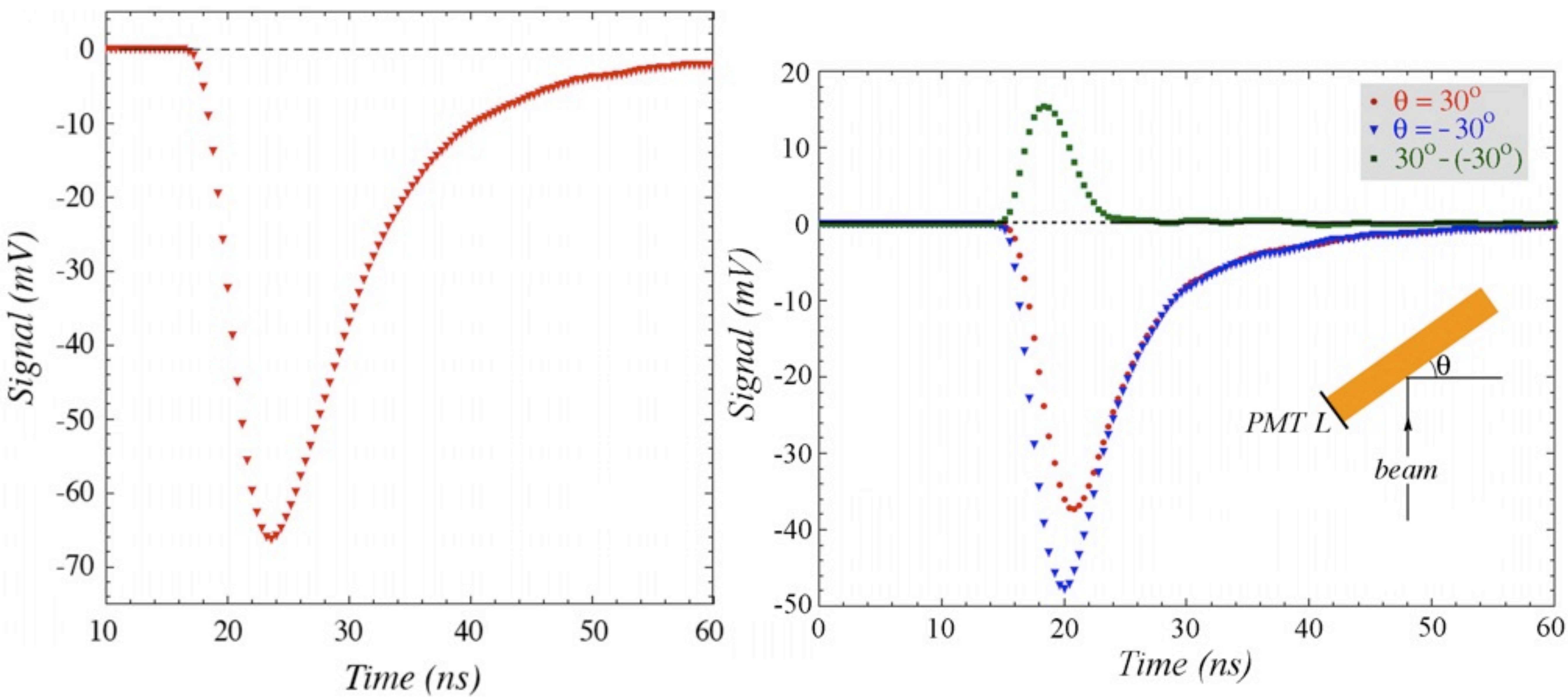

Figure 12: Average time structure of the signals measured with the PMT reading out one end (L) of a $PbWO_4$ crystal traversed by 10 GeV electrons, for two different orientations of the crystal, and the difference between these two time distributions. At $\theta = -30°$, Čerenkov light contributes to the signals, at $\theta = 30°$, it does not [14, 15]. When the crystal was read out from the other side, the prompt excess signal was detected for $\theta = 30°$, and was absent for $\theta = -30°$ [15].

Lead Tungstate ($PbWO_4$) - III

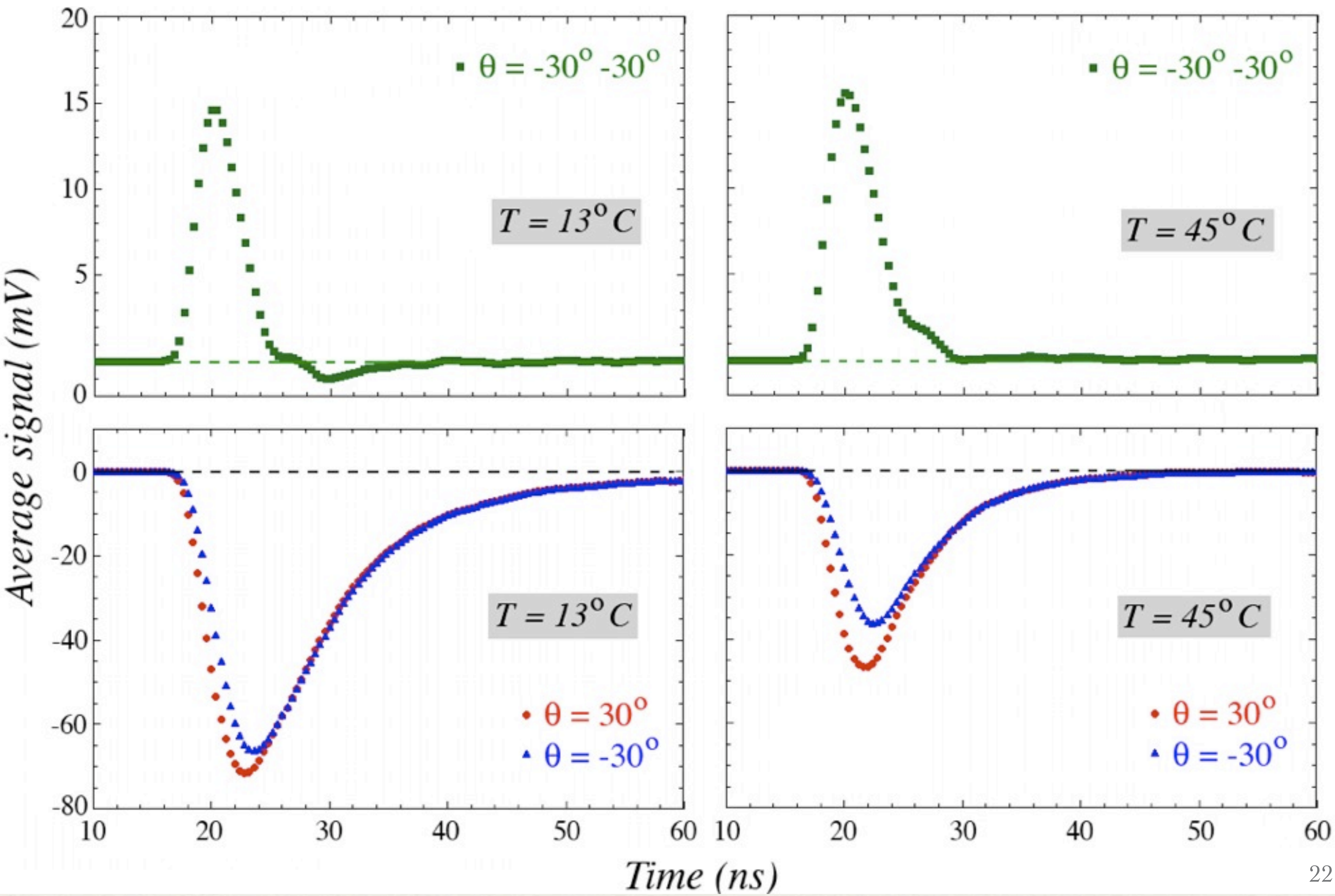

Lead Tungstate ($PbWO_4$) - IV

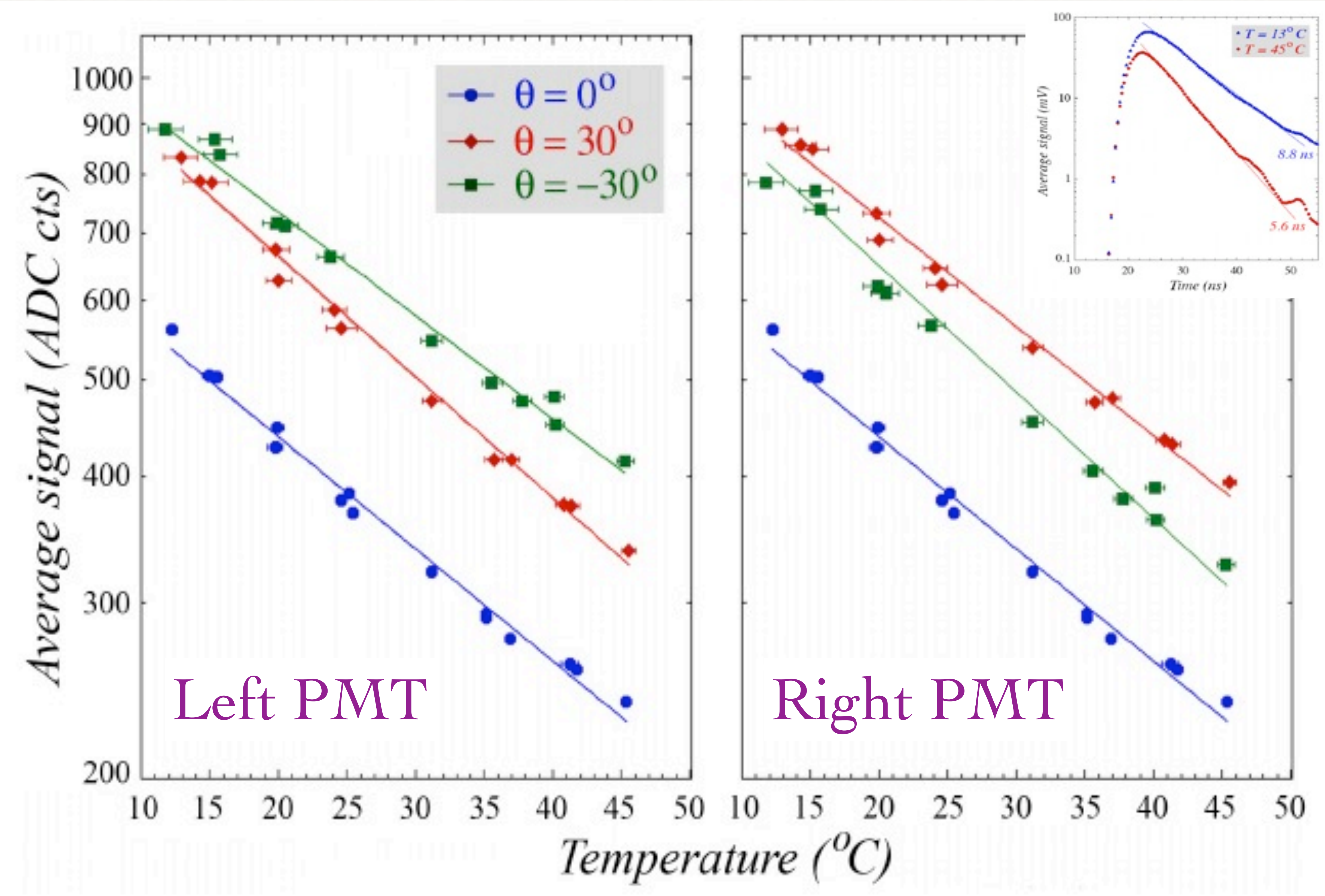

Lead Tungstate ($PbWO_4$) - V

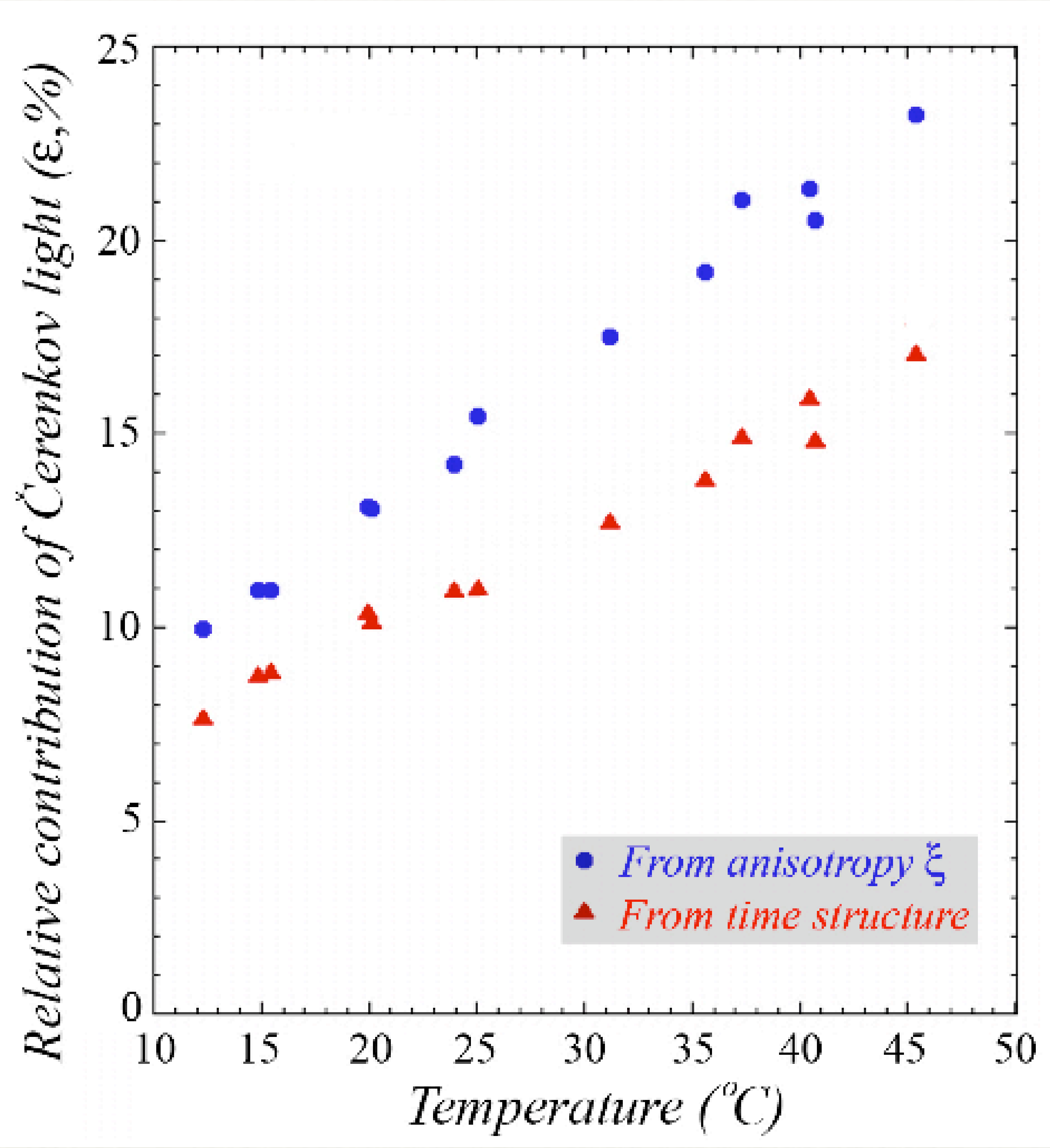

It is important to quantify the relative Cherenkov light contribution to the total light output. This is done in two ways on the left plot.

$$\xi(\theta) = \left|\frac{R_\theta - R_{-\theta} - L_\theta + L_{-\theta}}{R_\theta + R_{-\theta} + L_\theta + L_{-\theta}}\right|$$

BGO - I

- Advantages:
  - Scintillation spectrum peaks at 480 nm allowing the possibility of use of optical filters
  - Scintillation decay time is long (~300 ns) allowing easier discrimination against prompt Cherenkov light
- Disadvantages:
  - Brighter scintillator compared to $PbWO_4$ (C/S is about 100 times smaller)

BGO - II

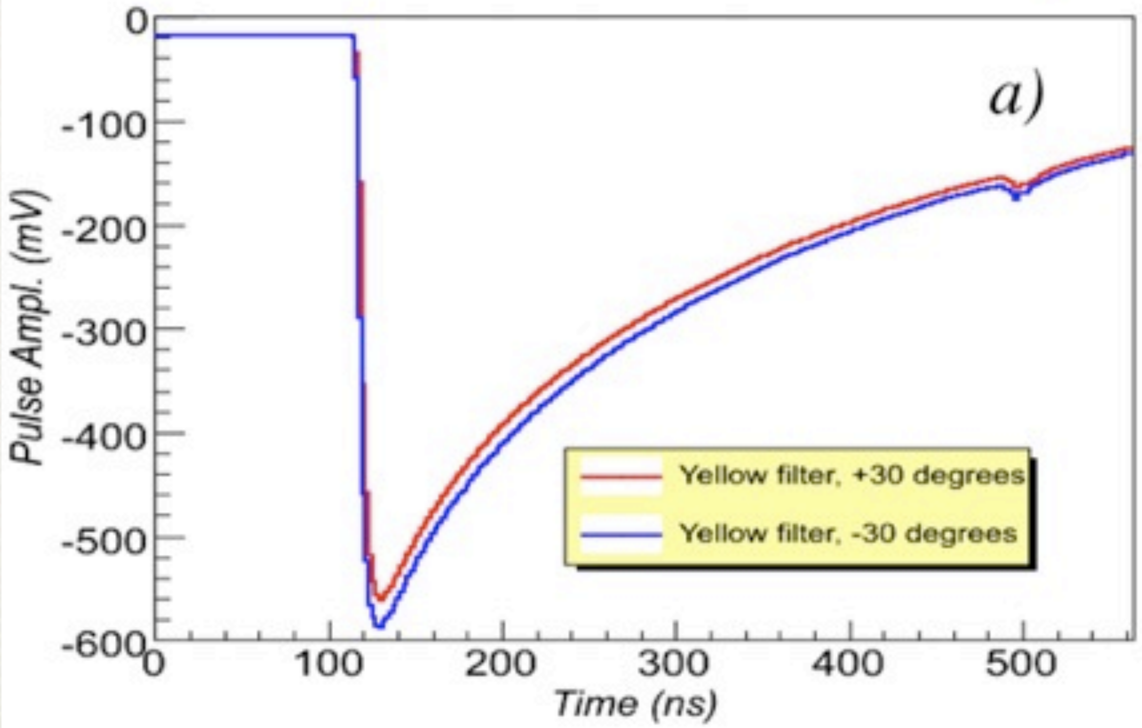
a)
Pulse Ampl. (mV)
Time (ns)
Yellow filter, +30 degrees
Yellow filter, -30 degrees

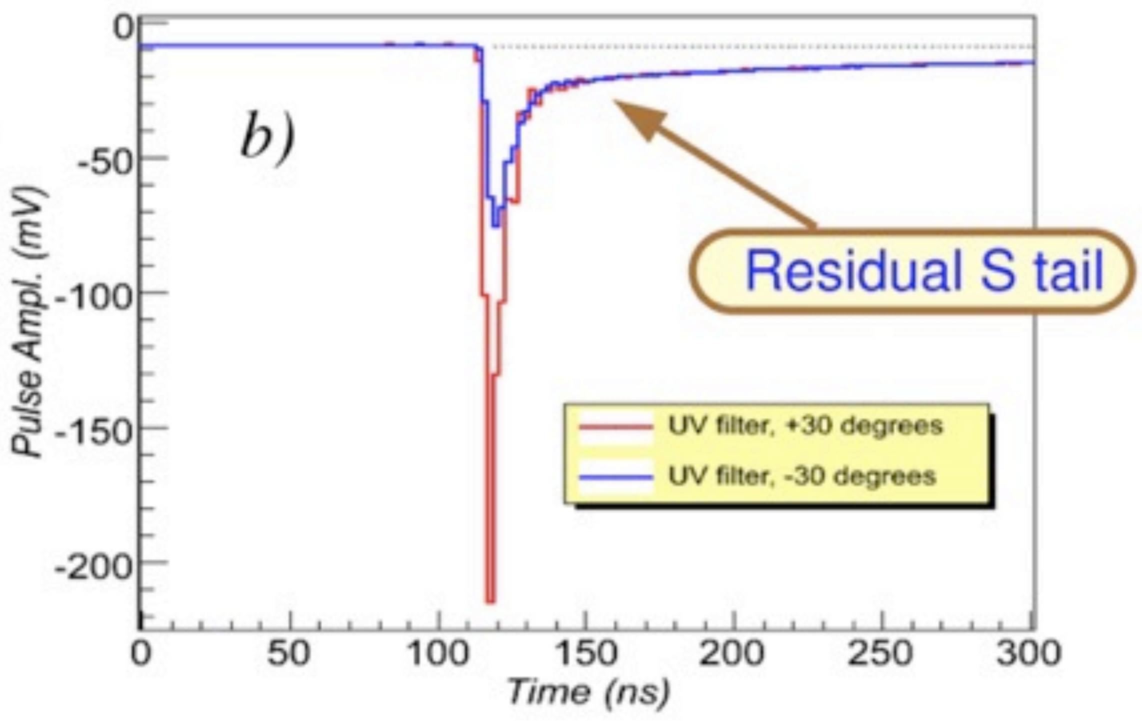
b)
Pulse Ampl. (mV)
Time (ns)
Residual S tail
UV filter, +30 degrees
UV filter, -30 degrees

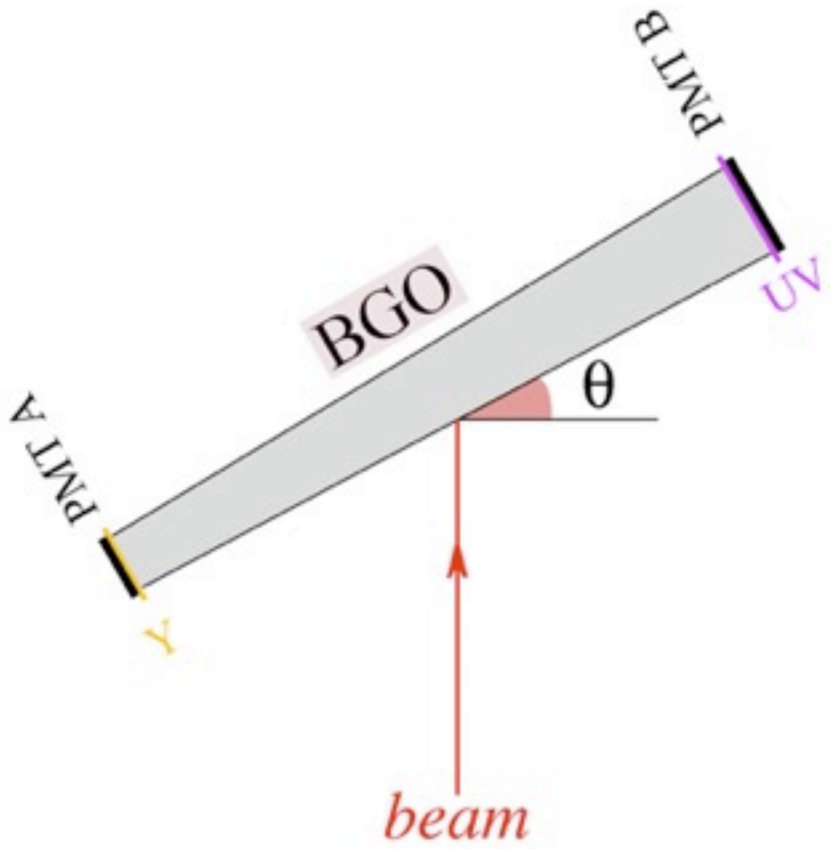
PMT B
UV
BGO
θ
PMT A
Y
beam

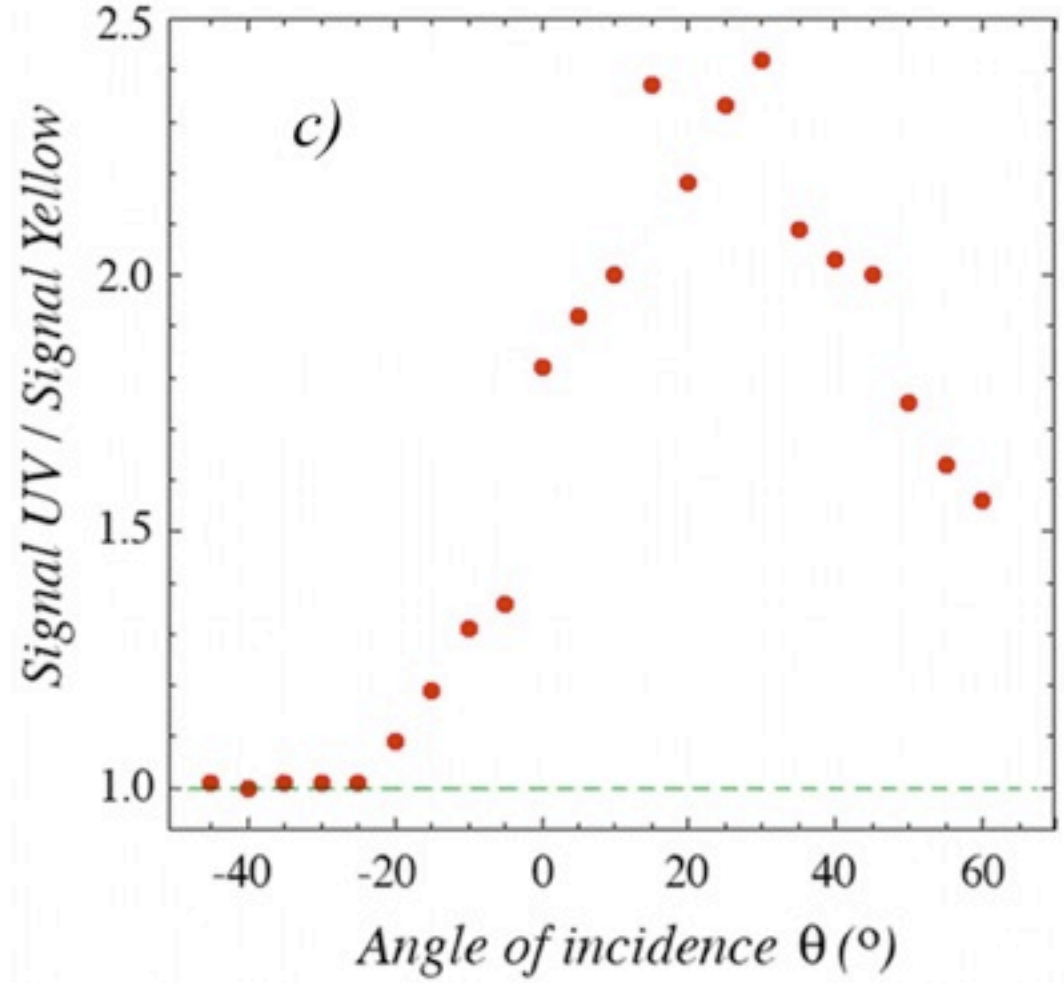
c)
Signal UV / Signal Yellow
Angle of incidence θ (°)

BGO - III

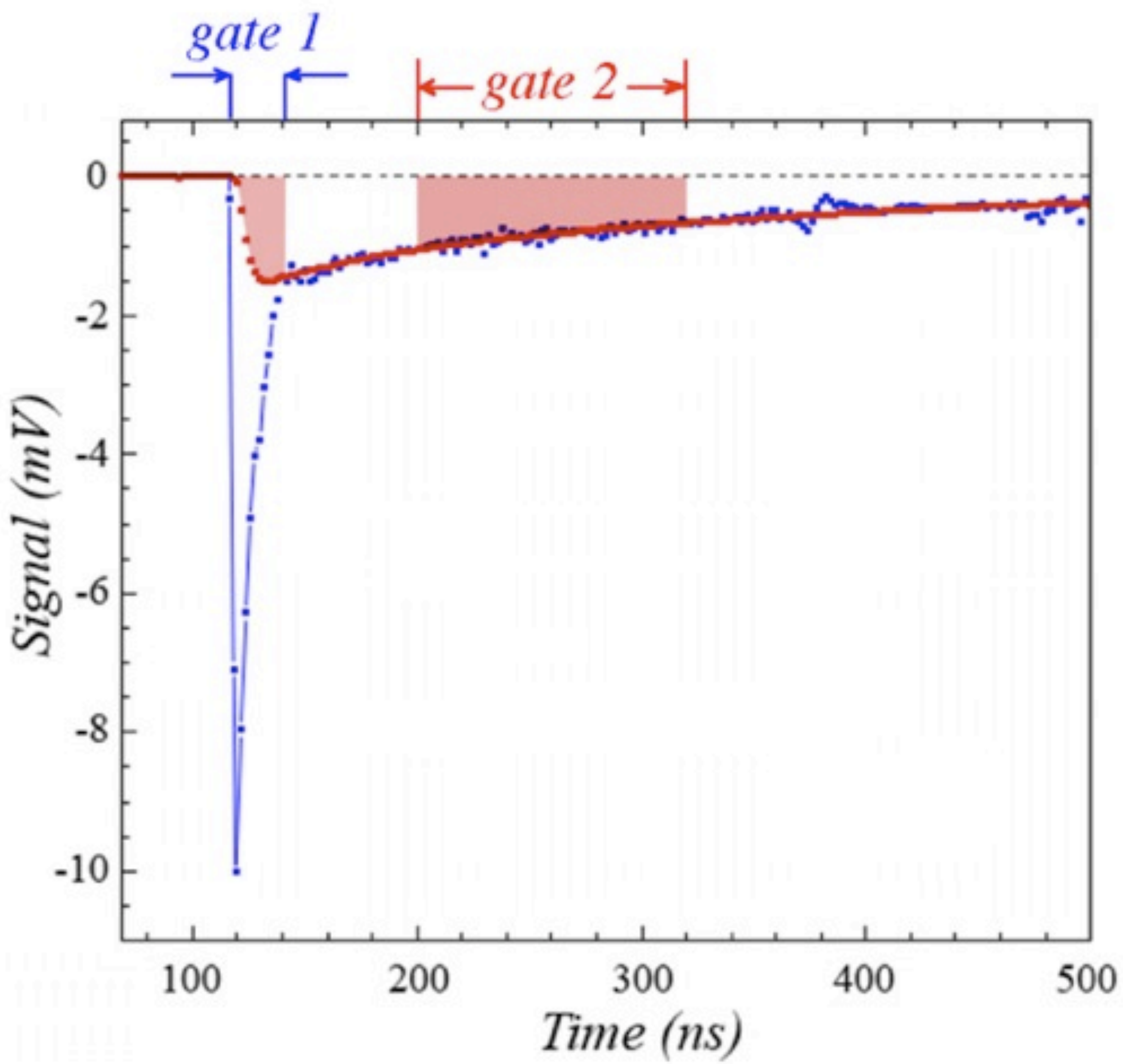

Figure 14: The time structure of a typical shower signal measured in the BGO em calorimeter equipped with a UV filter. These signals were measured with a sampling oscilloscope, which took a sample every 0.8 ns. The UV BGO signals were used to measure the relative contributions of scintillation light (gate 2) and Čerenkov light (gate 1) [15].

BGO - IV

Figure 15: The calorimeter during installation in the H4 test beam, which runs from the bottom left corner to the top right corner in this picture. The 100-crystal BGO matrix is located upstream of the fiber calorimeter, and is read out by 4 PMTs on the left (small end face) side.

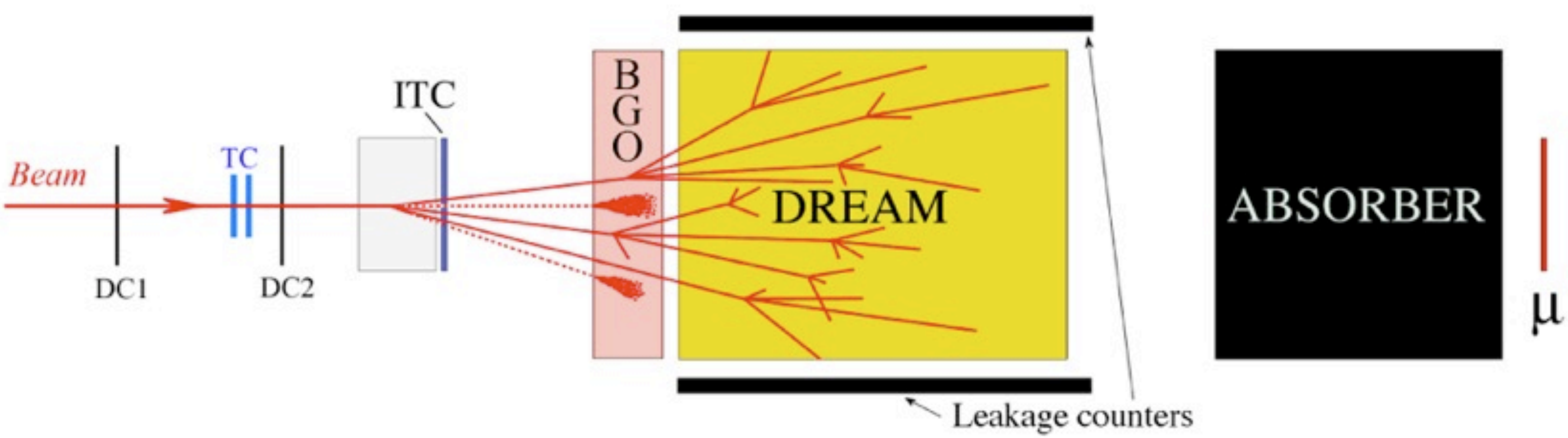

BGO - V

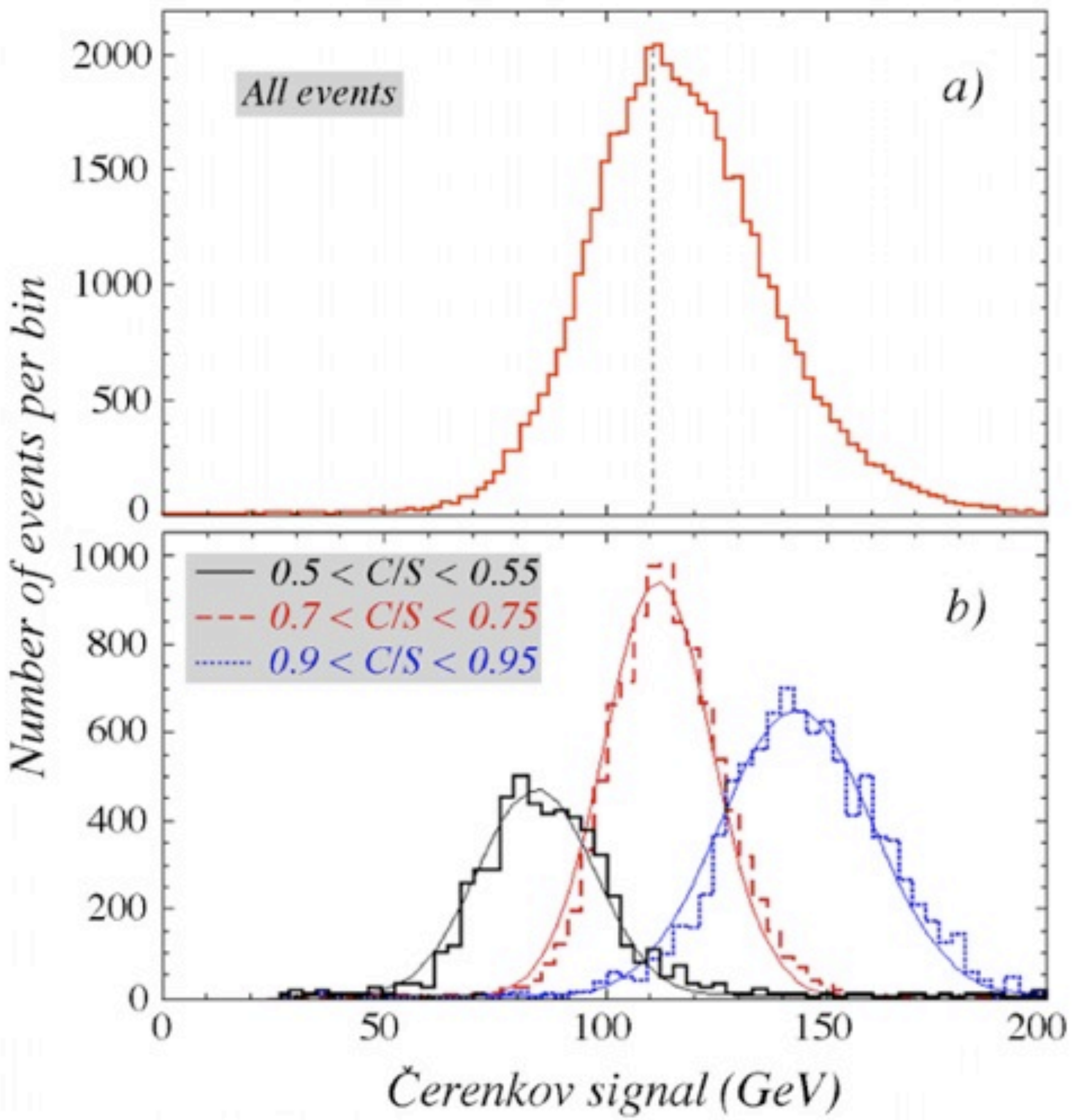

On average, ~50% of the "jet" energy deposited in BGO matrix

200 GeV "jets"

Figure 17: The Čerenkov signal distribution for 200 GeV "jet" events detected in the BGO + fiber calorimeter system (a) together with the distributions for subsets of events selected on the basis of the ratio of the total Čerenkov and scintillation signals in this detector combination (b) [17].

Correlations between Crystal(s) and DREAM Module

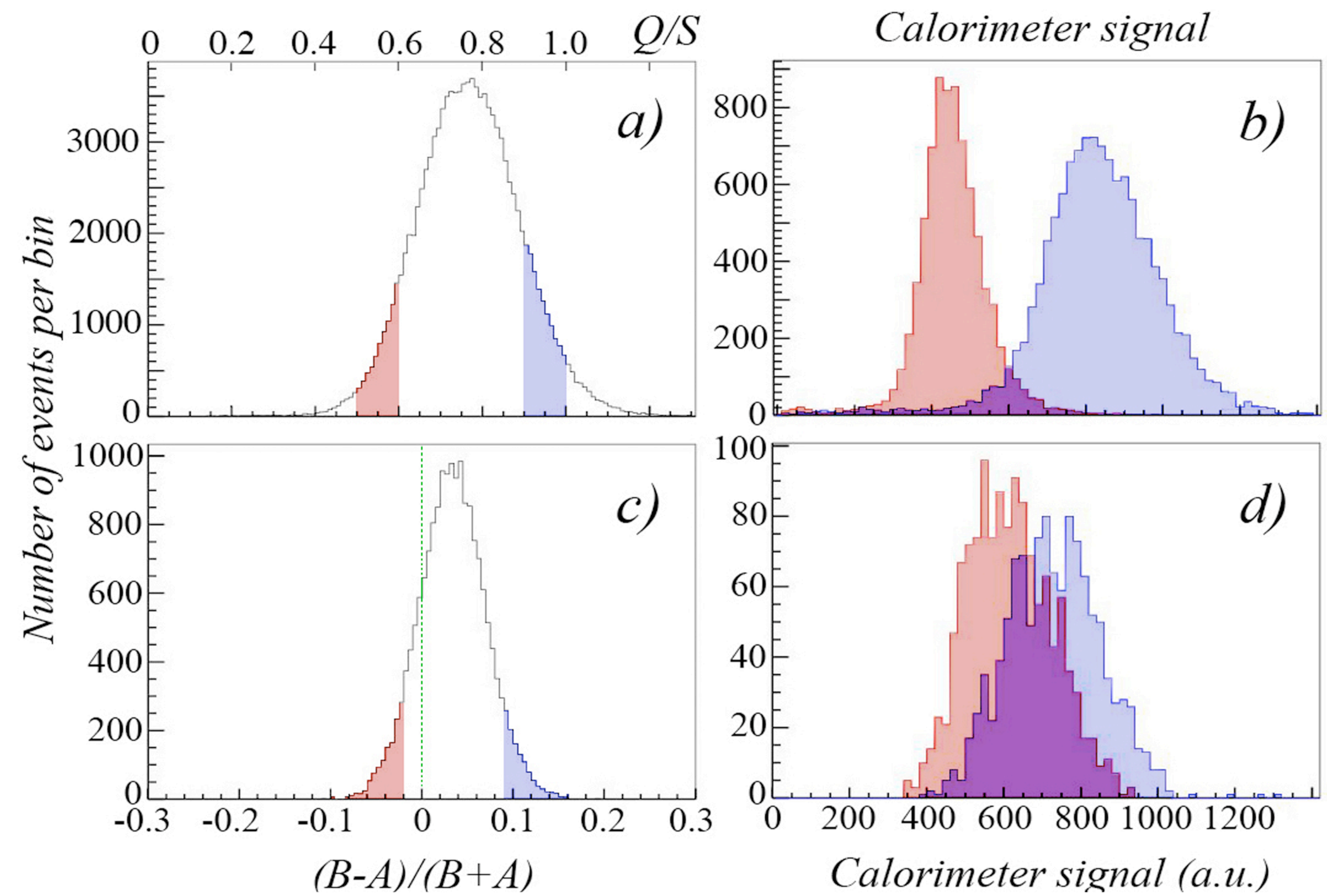

DREAM stand-alone (2 separate media)

$PbWO_4$ matrix (directionality)

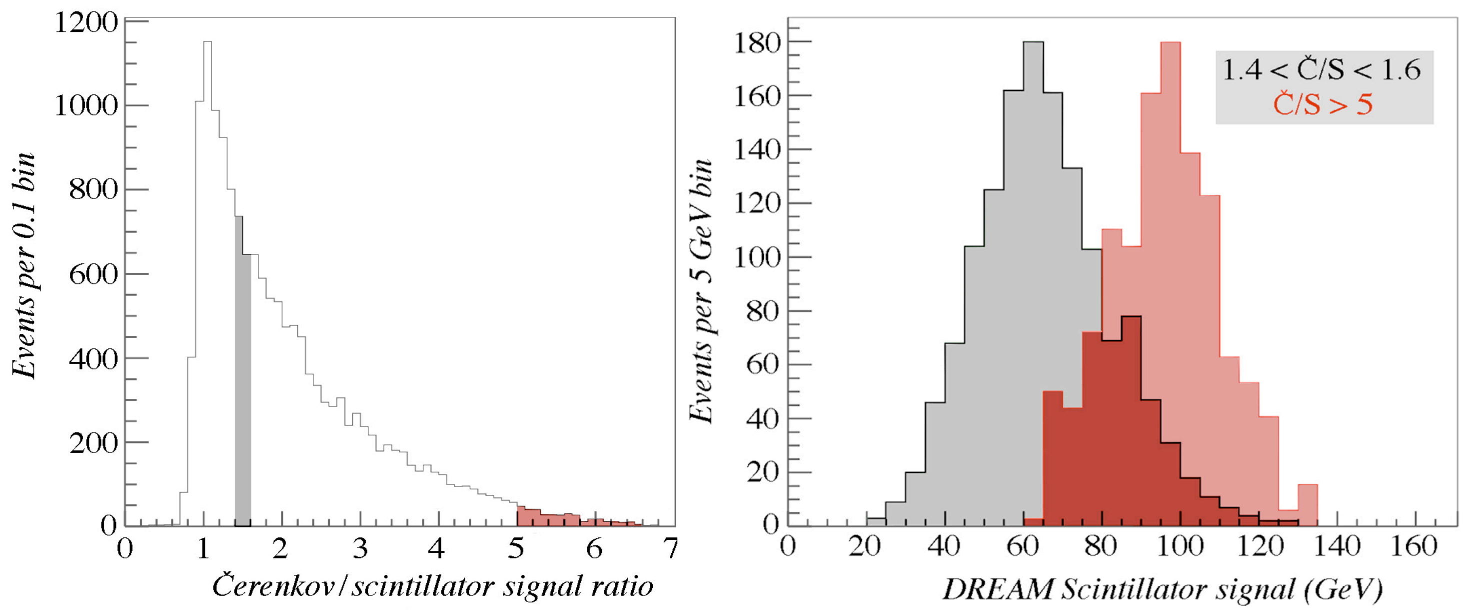

BGO_{UV} (1 crystal)

(time structure + spectrum)

$PbWO_4$ *vs* BGO

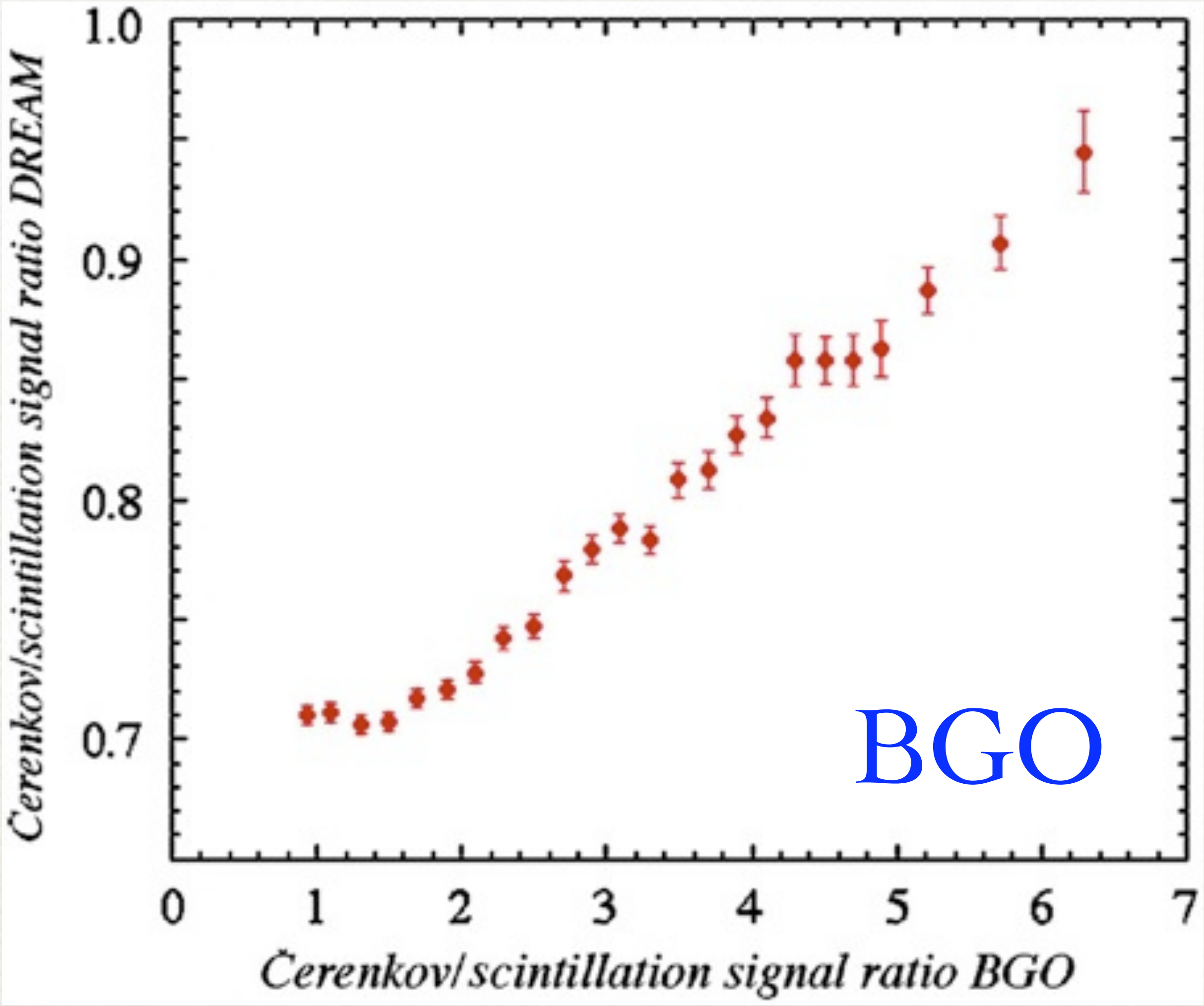

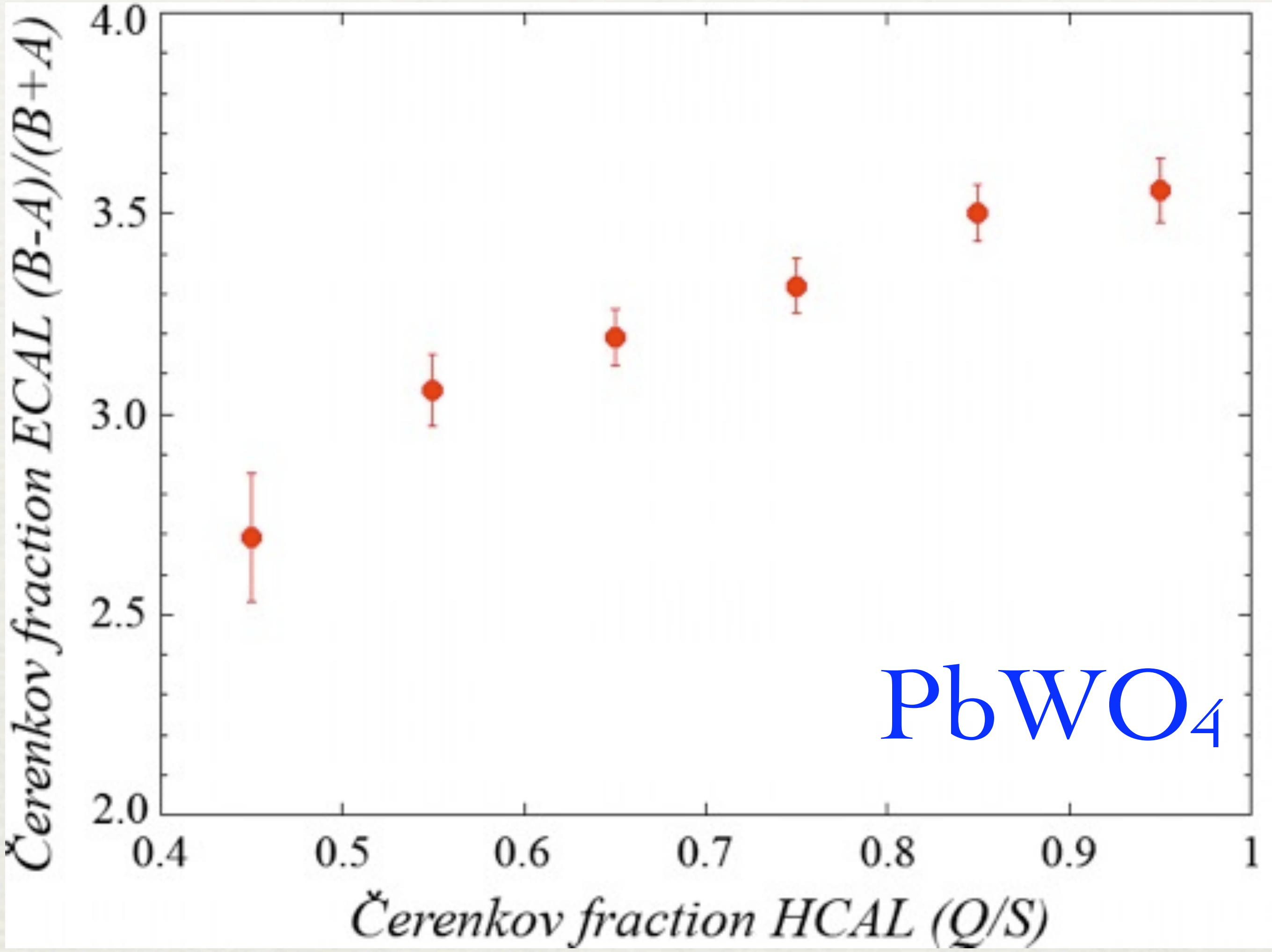

- Neither crystal is ideal although it is easier to work with BGO as evidenced by a stronger correlation in a wider dynamic range between the crystals and the DREAM module.

Correlations between BGO and DREAM Module

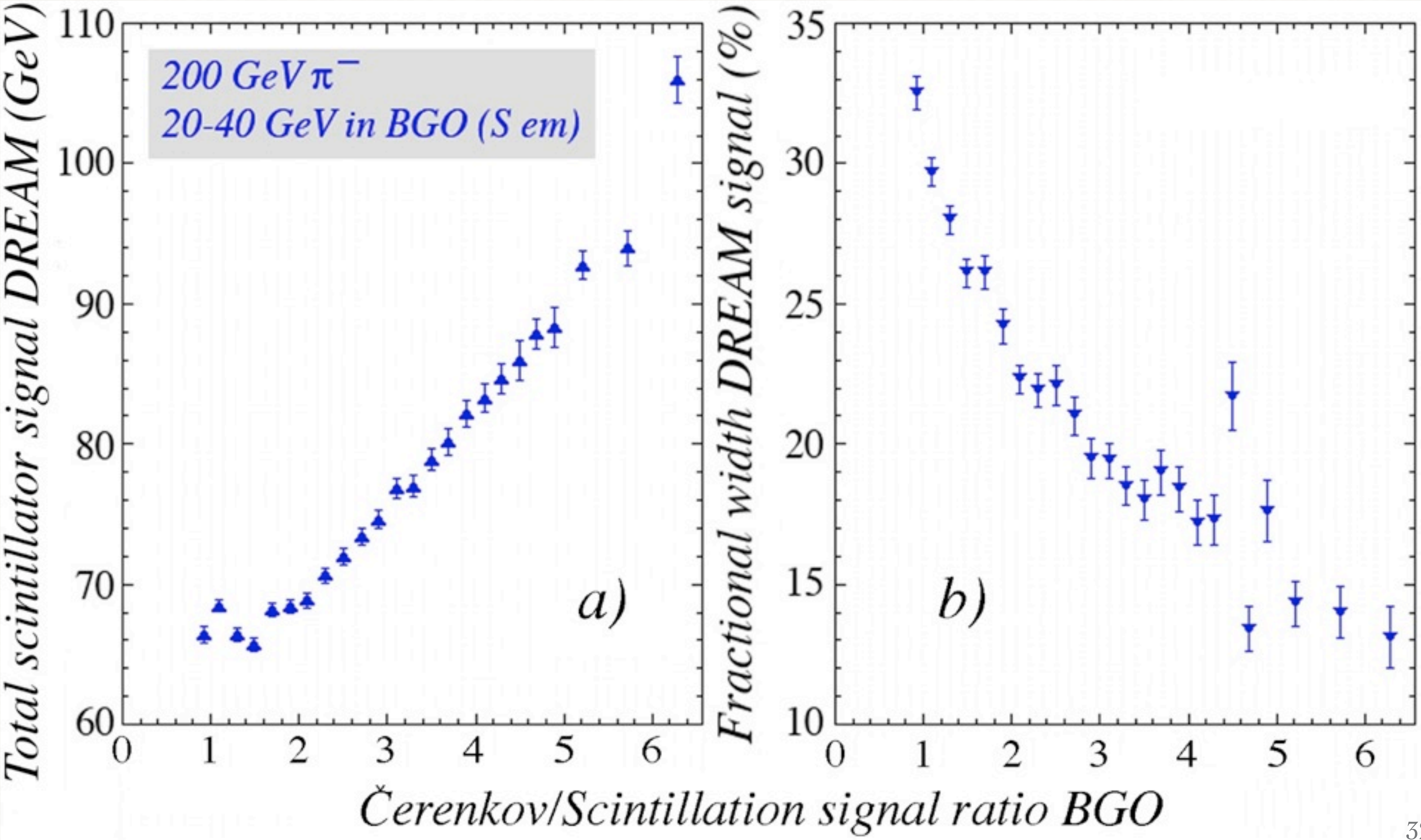

DREAM Crystal ?

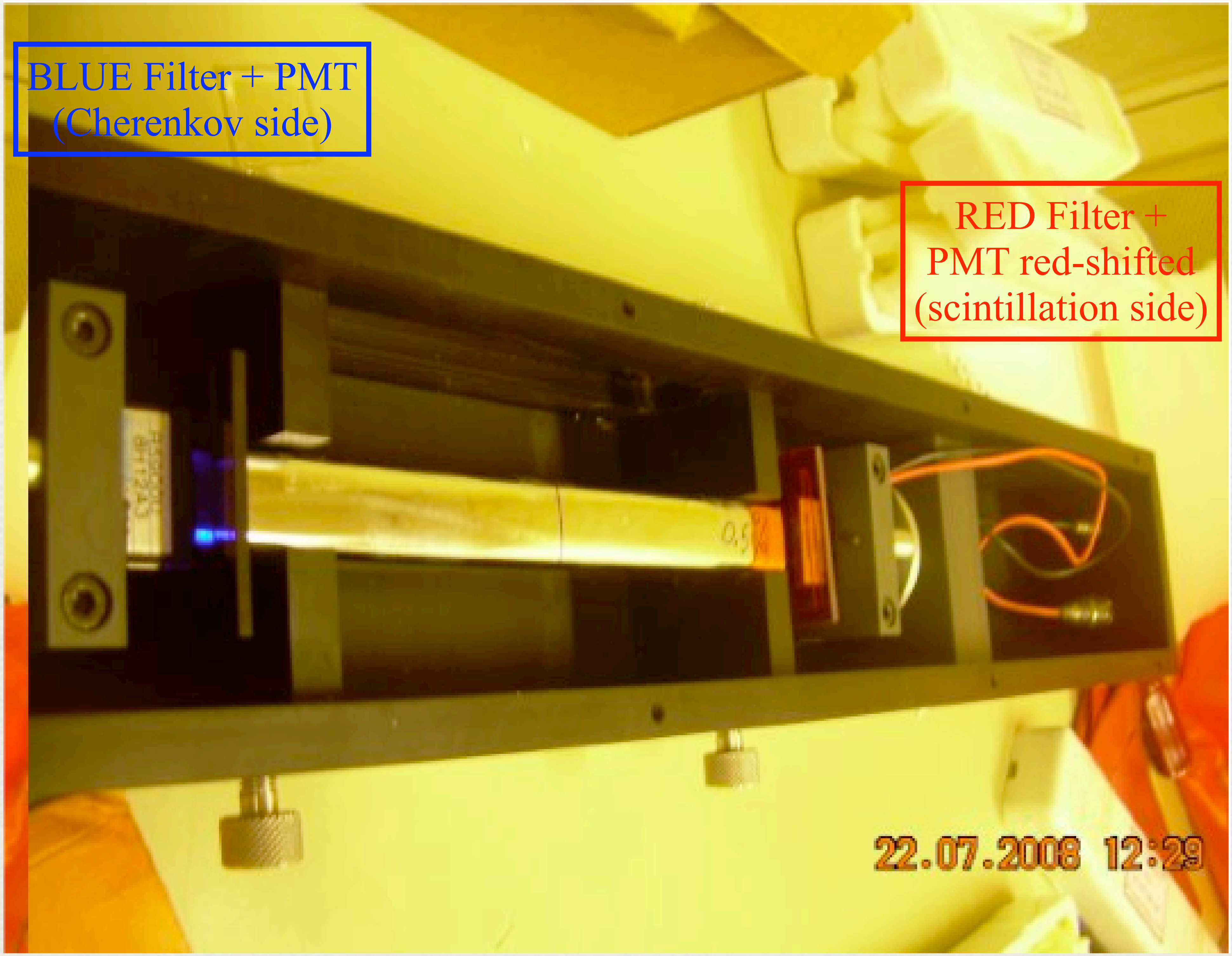

DREAM Crystal: Simple Strategy

Dope $PbW0_4$ in such a way that scintillation emission takes place at higher wavelengths with longer decay times (recall BGO example).

Two possibilities were identified as a starting point by the experts (Bicocca-Milan, Minsk and Prague)

- Molybdenum (1%, 5%; 0.1%, 0.2%, 0.3%)
- Praseodymium (0.5%, 1%, 1.5%)

$PbWO_4$ + Mo Crystal

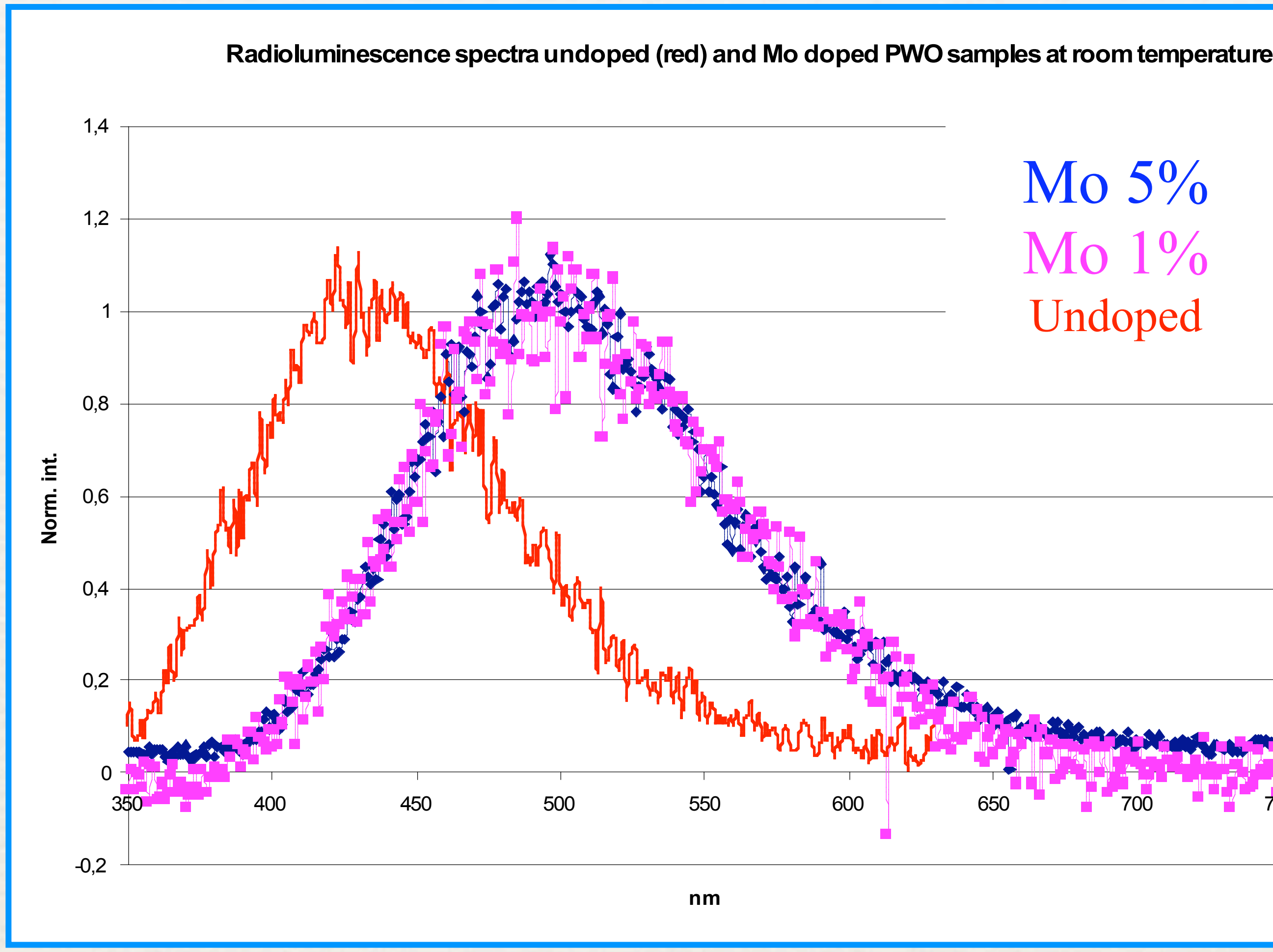

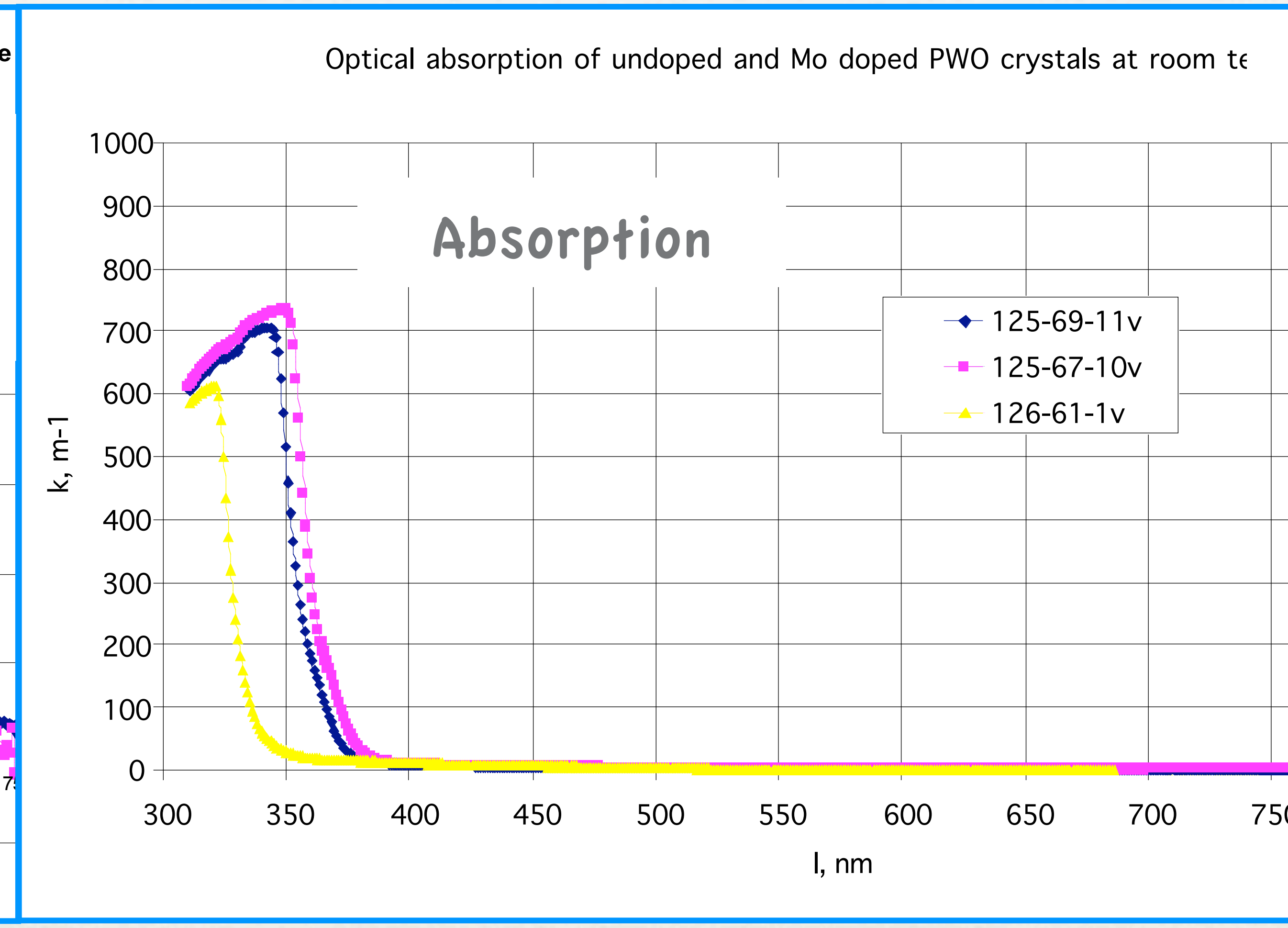

Doping lead tungstate with Molybdenum shifts the emission peak to longer wavelengths but also shifts the absorption edge.

$PbWO_4$ + 1% Mo Crystal

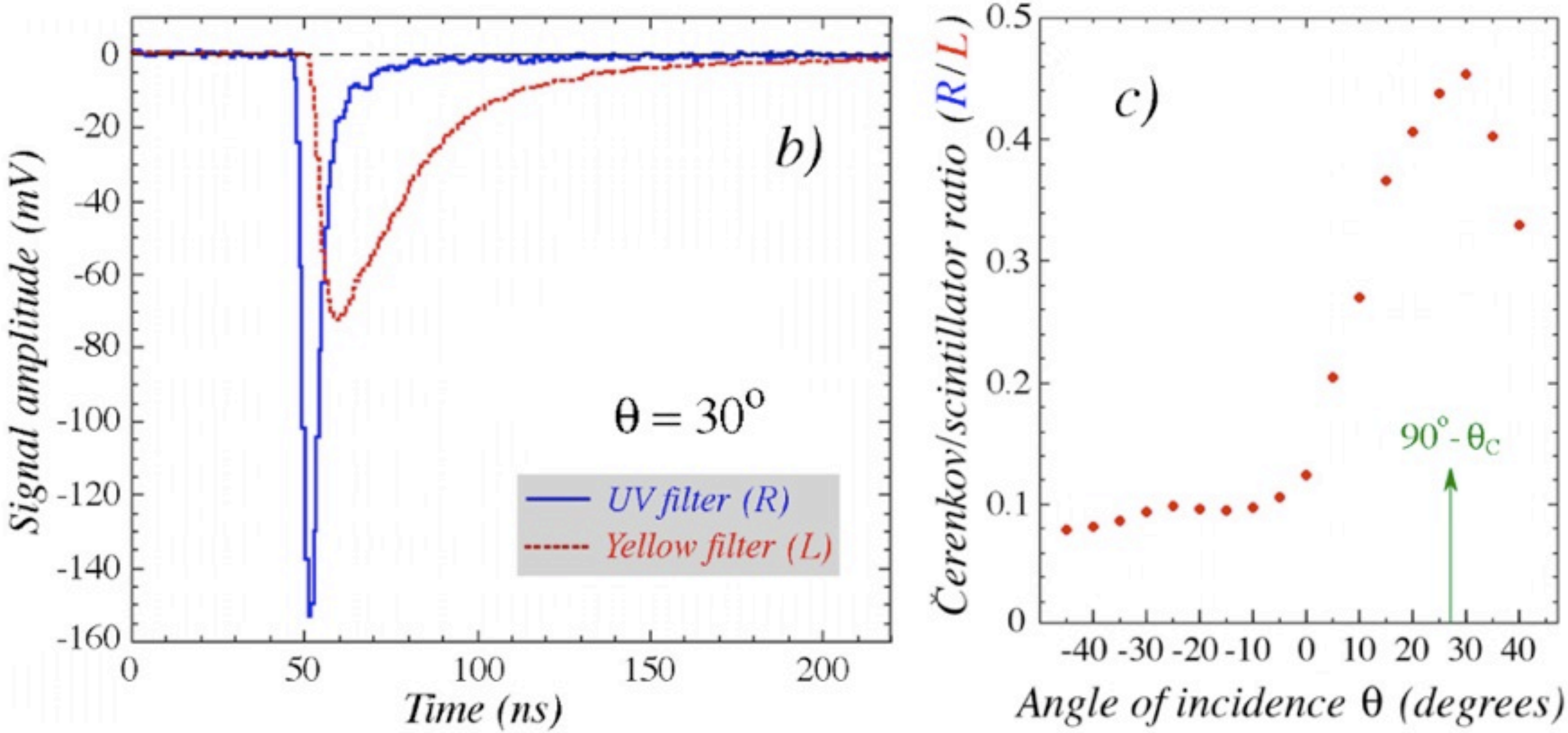

Figure 3: Unraveling of the signals from a Mo-doped $PbWO_4$ crystal into Čerenkov and scintillation components. The experimental setup is shown in diagram *a*. The two sides of the crystal were equipped with a UV filter (side *R*) and a yellow filter (side *L*), respectively. The signals from 50 GeV electrons traversing the crystal are shown in diagram *b*, and the angular dependence of the ratio of these two signals is shown in diagram *c* [6].

$PbWO_4$ + 1% Mo Crystal

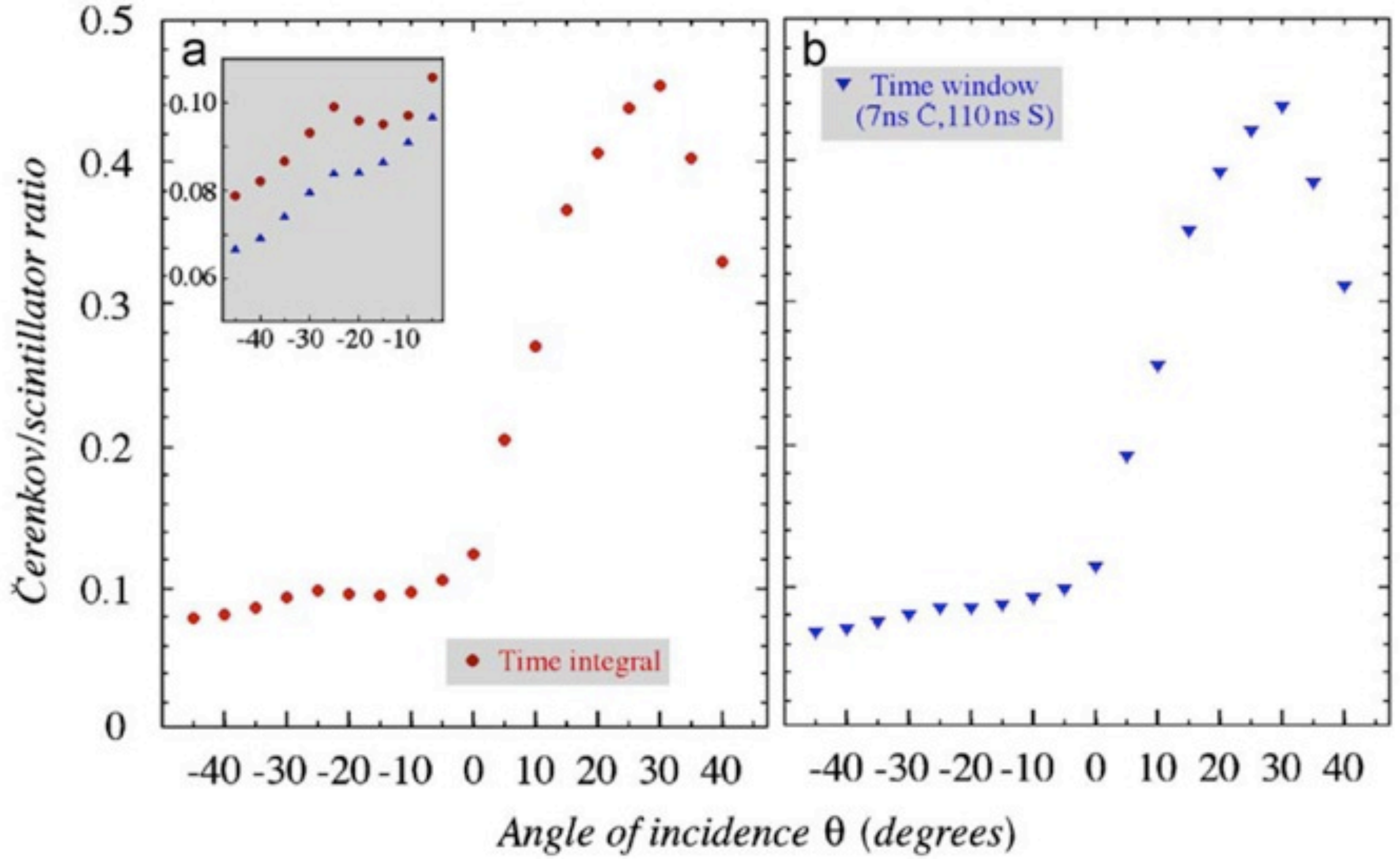

Fig. 9. Ratio of the signals from the light transmitted by the UV and the yellow filters, as a function of the angle of incidence of the beam particles (50 GeV e^-). The signals were obtained either by integrating over the entire time structure (a), or over limited time intervals chosen such as to purify their Cherenkov or scintillation content (b). The insert shows a blown-up version of the data at $\theta < 0$.

pulse shape information

t = 48-55 ns (contains more than 90% of the signal) for C

t = 70-180 ns for S

$PbWO_4$ + 1% Mo Crystal

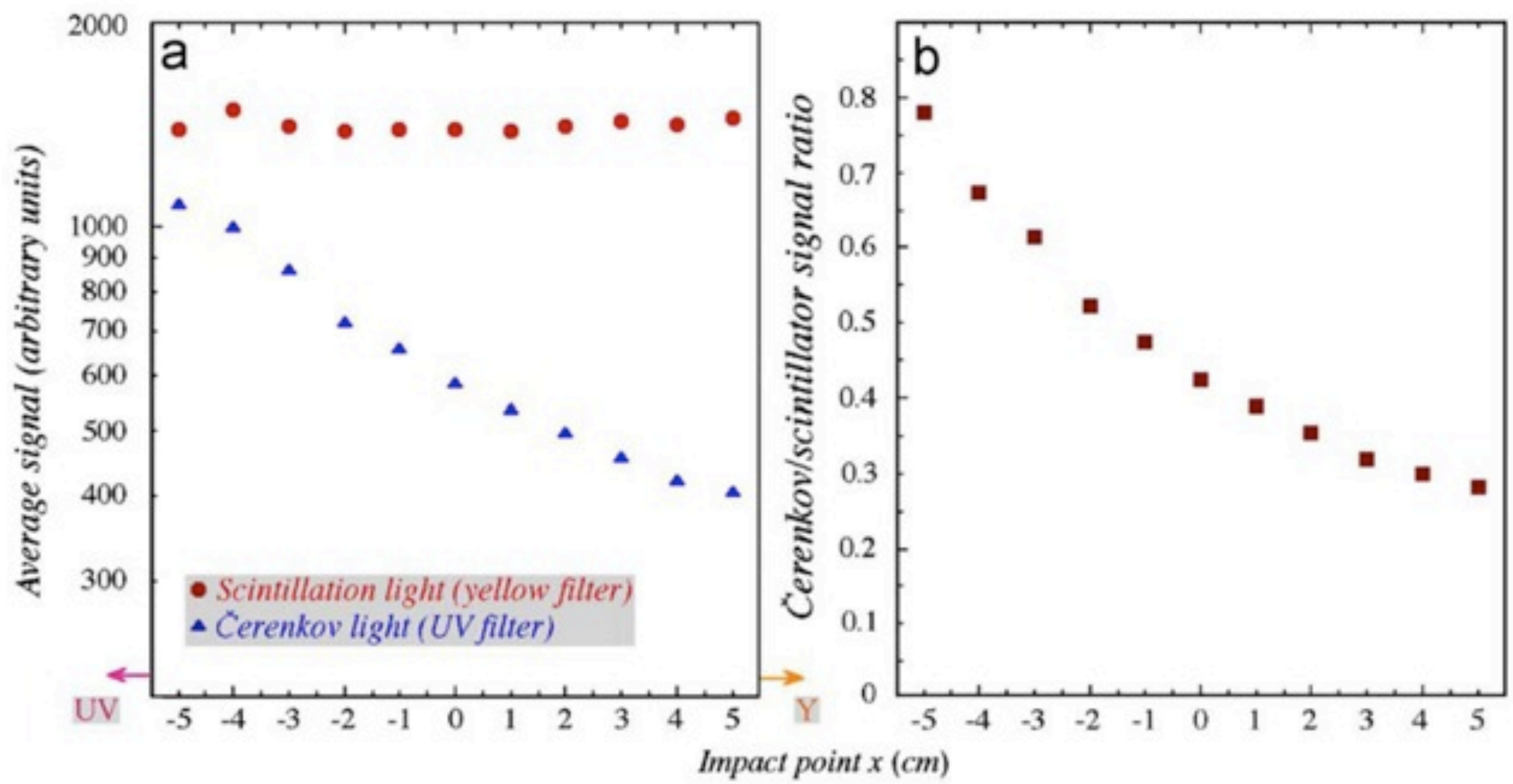

Fig. 10. Average signal from 50 GeV electrons in the $PbWO_4$ crystal doped with 1% Mo, as a function of the impact point of the particles. Shown are the signals generated by the light passing the UV and yellow filters, respectively, (a), and the ratio of these signals (b). The positions of these filters (UV,Y) are indicated.

Drawbacks:

- strong self-absorption
- poor light-yield (8 ±1 pe/GeV)

$PbWO_4$ + Mo Crystal (0.1%, 0.2%, 0.3%)

With a lower Mo concentration it is possible to:

1. maintain the shift of the scintillation emission spectrum to higher λ with respect to undoped $PbWO_4$
2. reduce the shift of the absorption cut-off to higher λ with respect to higher Mo concentration

Combination of these features with higher QE PMT and better suitable filters should allows to achieve a good C/S ratio without light attenuation.

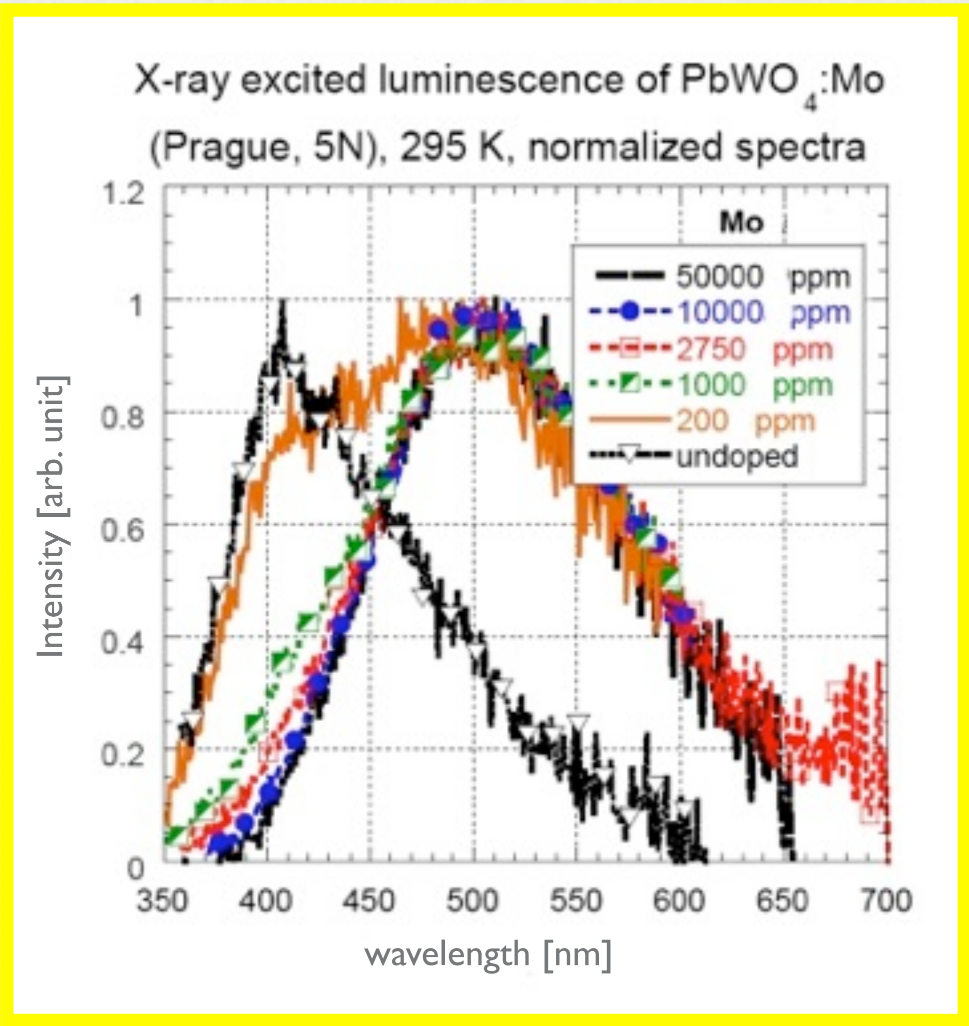

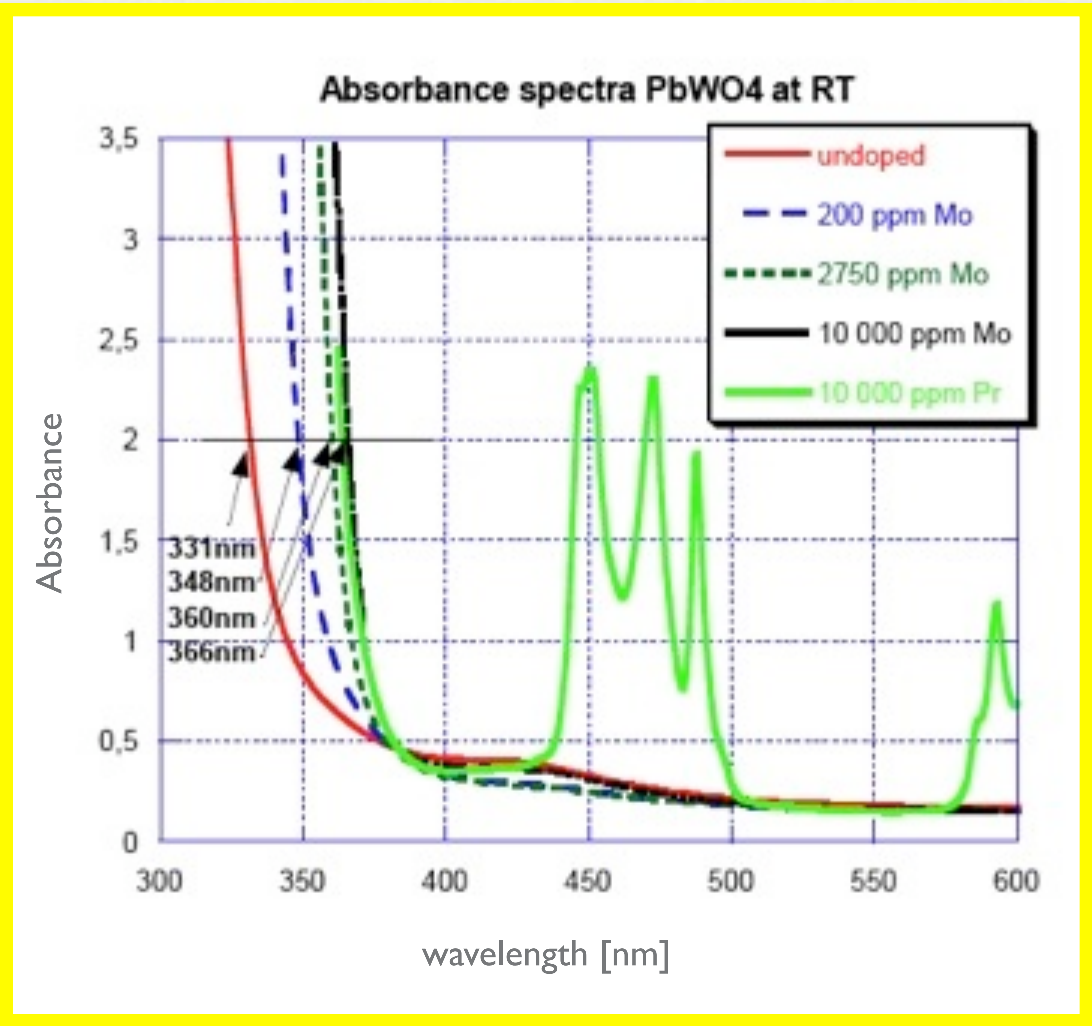

What about Neutrons?

- ~95% of neutrons are created by nuclear deexication with average energy of ~ 3 MeV
- These neutrons lose their energy mostly through multiple elastic scattering
- Energy loss goes like A^{-1}, so protons dominate
- np cross sections are large 2b(3 MeV) and 12b(0.1 MeV)
- Mean free path between np scattering is 56 cm to 10 cm
- Average time between np scattering is ~23 ns (expect exponential tail in time structure)
- Kinetic energy of neutrons reduced by 1/e in 33 ns if all other processes are insignificant
- ...

Neutron Tail

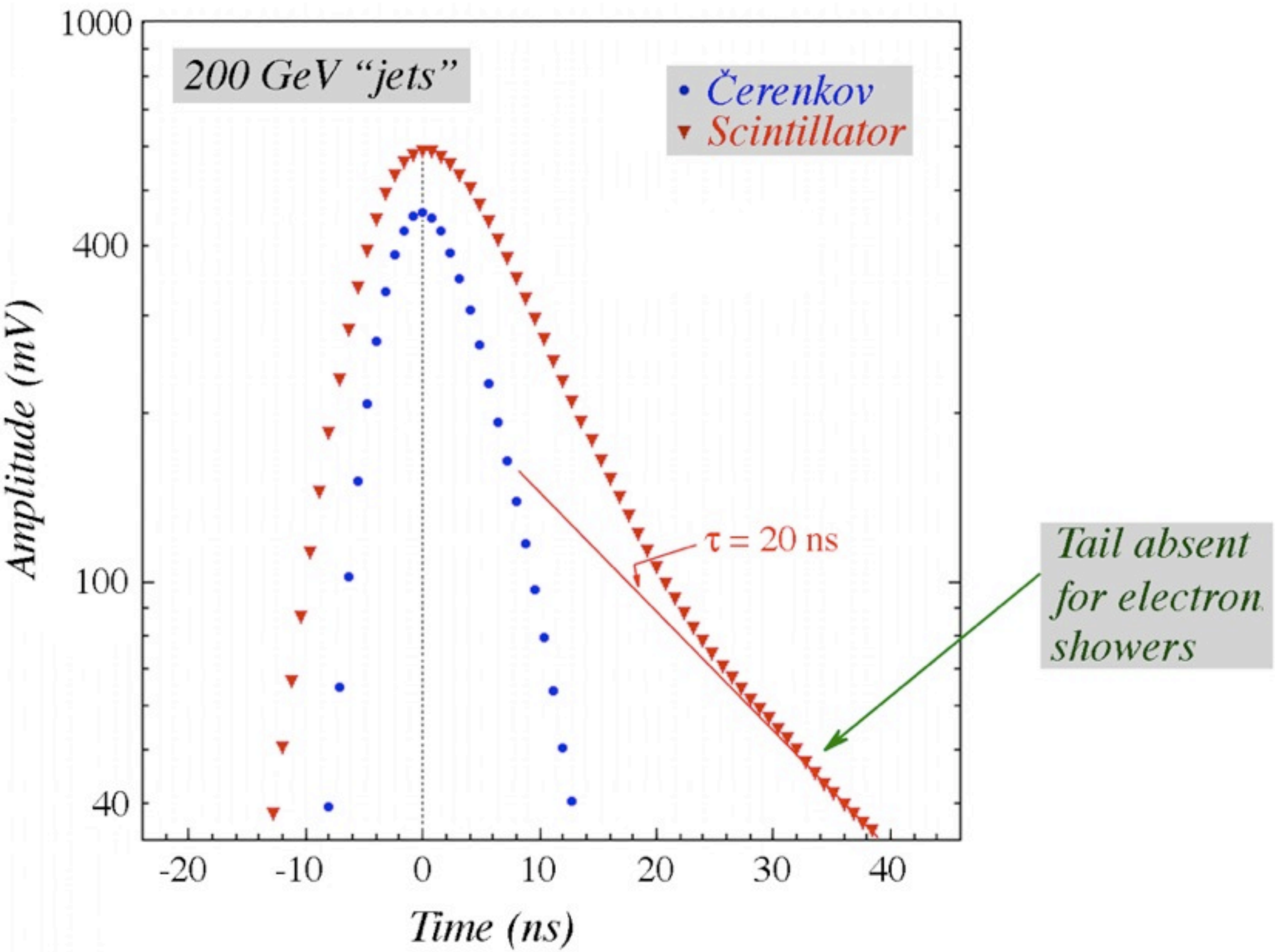

Neutron and EM Fractions

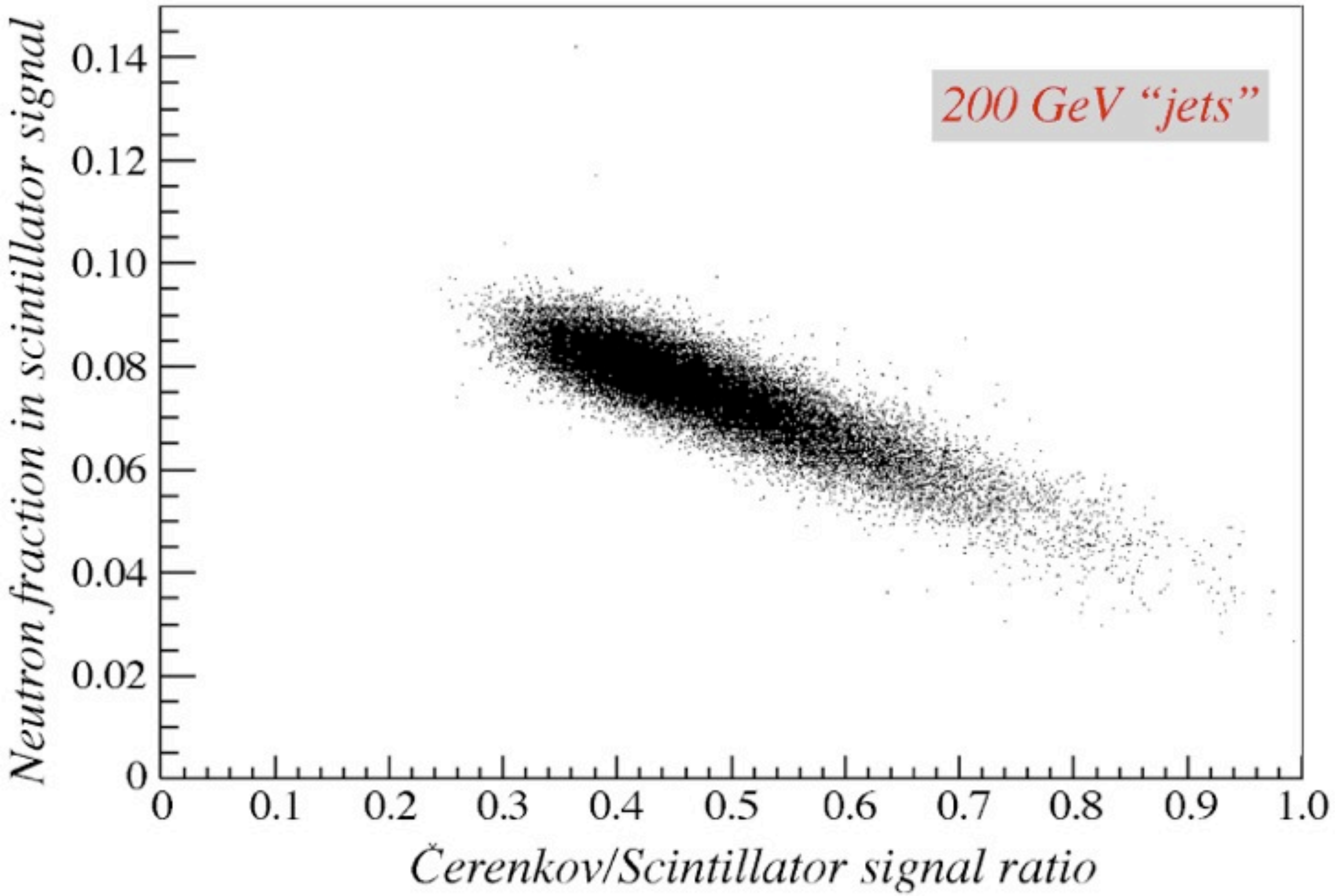

Figure 4: Scatter plot of the fraction of the scintillation light contained in the (20 ns) exponentional tail versus the Čerenkov/scintillation signal ratio measured in these events [9].

Neutron Fractions in Signal

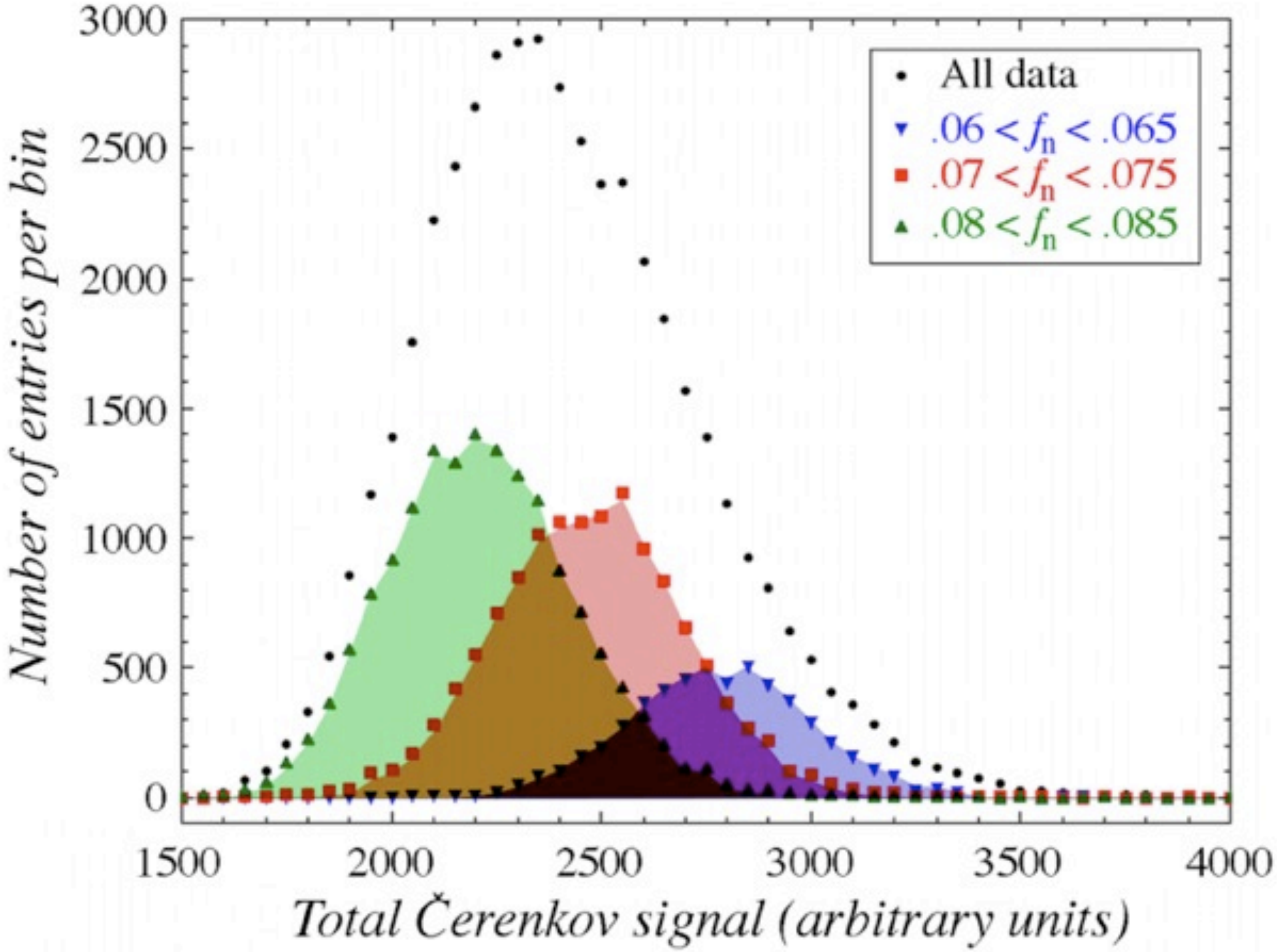

Figure 18: Distribution of the total Čerenkov signal for 200 GeV "jets" and the distributions for three subsets of events selected on the basis of the fractional contribution of neutrons to the scintillator signal [9].

Neutron Fraction & Energy Resolution

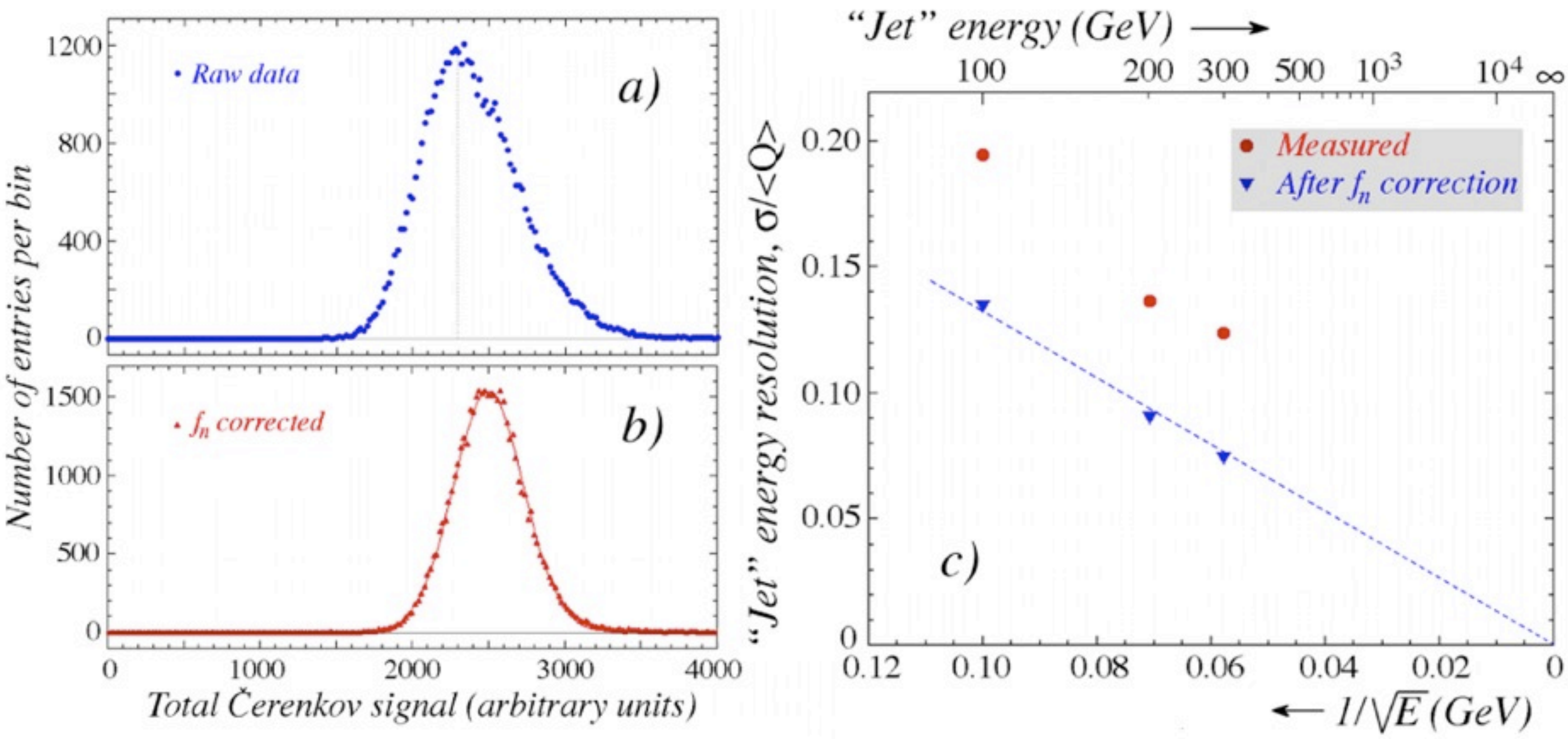

Figure 19: Distribution of the total Čerenkov signal for 200 GeV "jets" before (*a*) and after (*b*) applying the correction based on the measured value of f_n, described in the text. Relative width of the Čerenkov signal distribution for "jets" as a function of energy, before and after a correction that was applied on the basis of the relative contribution of neutrons to the scintillator signals (*c*) [9].

What's Next?

- Analyze 2009 data (lower Mo concentrations in lead tungstate, large BGO matrix, 5Msample/s digitization rate, leakage measurements, improved neutron data, *etc.*)
- Fluctuations in the em and neutron energy are under control
- Fluctuation in Cherenkov light yield and sampling need improvement (dedicated crystals and other ideas...)
- Build a sizable and scalable unit